HHS Public Access

Author manuscript

Immunity. Author manuscript; available in PMC 2021 October 13.

Published in final edited form as:

Immunity. 2020 October 13; 53(4): 793–804.e9. doi:10.1016/j.immuni.2020.08.002.

IgE effector mechanisms, in concert with mast cells, contribute to acquired host defense against *S. aureus*

Philipp Starkl[1,2,3,14,*], **Martin L. Watzenboeck**[1,2], **Lauren M. Popov**[4,5], **Sophie Zahalka**[1,2], **Anastasiya Hladik**[1,2], **Karin Lakovits**[1,2], **Mariem Radhouani**[1,2], **Arvand Haschemi**[6], **Thomas Marichal**[3,7], **Laurent L. Reber**[3,8], **Nicolas Gaudenzio**[3,9], **Riccardo Sibilano**[3,10], **Lukas Stulik**[11], **Frédéric Fontaine**[2], **André C. Mueller**[2], **Manuel R. Amieva**[4,12], **Stephen J. Galli**[3,4,10,13,*], **Sylvia Knapp**[1,2,13,*]

[1]CeMM - Research Center for Molecular Medicine of the Austrian Academy of Sciences, 1090 Vienna, Austria

[2]Laboratory of Infection Biology, Dept. of Medicine I, Medical University of Vienna, 1090 Vienna, Austria

[3]Dept. of Pathology, Stanford University School of Medicine, Stanford, CA, 94305-5176, USA

[4]Dept. of Microbiology and Immunology, Stanford University School of Medicine, Stanford, CA, 94305-5176, USA

[5]Dept. of Molecular and Cell Biology, University of California, Berkeley, CA, 94720, USA

[6]Dept. of Laboratory Medicine, Medical University of Vienna, 1090 Vienna, Austria

[7]GIGA-Research and Faculty of Veterinary Medicine, University of Liege, 4000 Liege, Belgium

[8]Center for Physiopathology of Toulouse-Purpan (CPTP), UMR 1043, University of Toulouse, INSERM, CNRS, 31024 Toulouse, France

[9]Unité de Différenciation Epithéliale et Autoimmunité Rhumatoïde (UDEAR), UMR 1056, INSERM, Université de Toulouse, 31059 Toulouse, France

[10]Sean N. Parker Center for Allergy and Asthma Research, Stanford University, Stanford, CA, 94305-5176, USA

[11]X4 Pharmaceuticals (Austria) GmbH, 1030 Vienna, Austria

[12]Dept. of Pediatrics, Stanford University School of Medicine, Stanford, CA, 94305-5176, USA

[*]Correspondence: philipp.starkl@meduniwien.ac.at (P.S.); sgalli@stanford.edu (S.J.G.); sylvia.knapp@meduniwien.ac.at (S.K.).

Author contributions

P.S. conceived of the project and designed and performed most experiments, compiled the data and wrote the paper with S.J.G. and S.K. S.J.G. and S.K. were involved in planning the study and the experimental design, and provided critical feedback, reagents and support. M.L.W., L.M.P, S.E.Z., A. Hladik, K.L., M.R., A. Haschemi, T.M., L.L.R., N.G., R.S., F.F. and A.C.M helped with experiments and data analysis. L.S. and M.R.A. helped with *S. aureus* experiments and provided critical reagents. All authors helped finalizing the manuscript.

Declaration of Interests

The authors declare no competing interests.

[13]These authors contributed equally

[14]Lead contact

Summary

Allergies are considered to represent mal-directed type 2 immune responses against mostly innocuous exogenous compounds. Immunoglobulin E (IgE) antibodies are a characteristic feature of allergies and mediate hypersensitivity against allergens through activation of effector cells, particularly mast cells (MCs). While any physiologic functions of this dangerous branch of immunity have remained enigmatic, recent evidence shows that allergic immune reactions can help to protect against the toxicity of venoms. Because bacteria represent a potent alternative source of toxins, we assessed the possible role of allergy-like type 2 immunity in antibacterial host defense. We discovered that the adaptive immune response against *Staphylococcus aureus* (SA) skin infection substantially improved systemic host defense against secondary SA infections in mice. Moreover, this acquired protection depended on IgE effector mechanisms and MCs. Importantly, our results reveal a previously unknown physiologic function of allergic immune responses, IgEs and MCs in host defense against a pathogenic bacterium.

Graphical Abstract

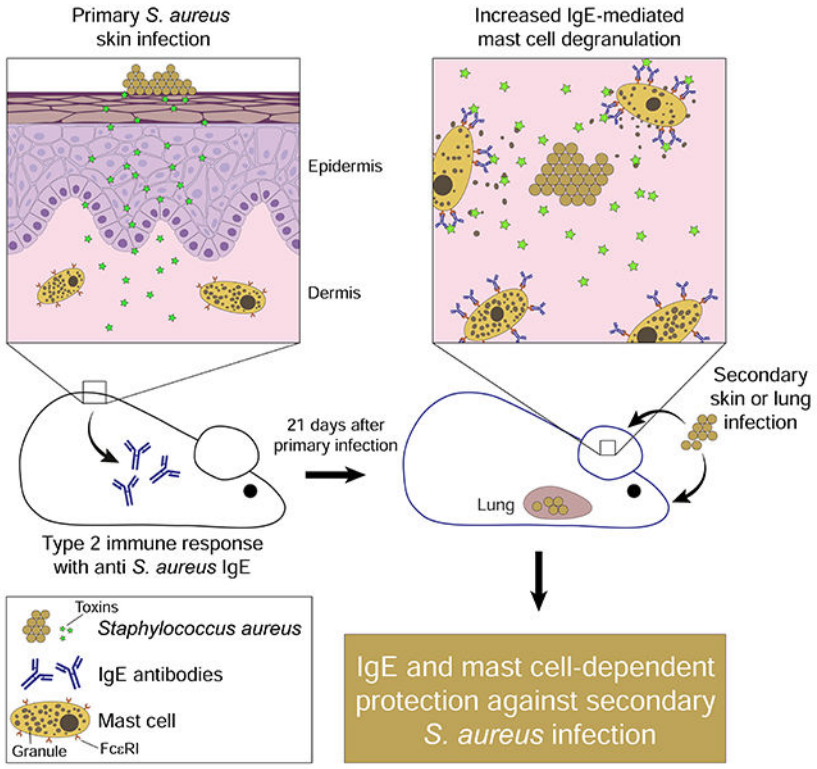

eTOC/In Brief

The biological functions of IgE antibodies and mast cells, critical components of allergic diseases, have been enigmatic. Starkl *et al.* here report a role for this *allergy module* of immunity in host defense against the bacterial pathogen *Staphylococcus aureus*.

Keywords

Allergy; allergy module; bacteria; basophils; degranulation; host defense; IgE; mast cells; *Staphylococcus aureus*; type 2 immunity

Introduction

Type 2 immune responses are characterized by the participation of T helper-2 cells, together with many other cell types including group 2 innate lymphoid cells, alternatively activated macrophages, eosinophils, basophils and mast cells (Gause et al., 2020). Such responses are induced during tissue remodeling, such as that following wounding, parasite infections or exposure to proteases or noxious substances (Gause et al., 2020; Harris and Loke, 2018; Lloyd and Snelgrove, 2018). However, type 2 immunity and its defining cytokines, such as interleukin-4 (IL-4) and IL-13, are also pre-requisites for allergic sensitization. Immunoglobulin (Ig)E is the prototypical antibody class produced during type 2 immune responses and mediates allergic reactions in sensitized individuals (Galli and Tsai, 2012). IgEs prime FcεRI-receptor-expressing cells, such as tissue-resident mast cells (MCs), thereby conferring antigen specificity and sensitivity, as well as defining their critical roles in allergic reactions (Galli and Tsai, 2012). While the contribution of such IgE-activated MCs to allergic diseases is well defined, the physiologic function of this immune module remains enigmatic (Oettgen, 2016).

We (Marichal et al., 2013; Starkl et al., 2016) and others (Palm et al., 2013) recently provided experimental evidence for the *toxin hypothesis*, that proposes allergic reactions constitute an important host defense mechanism against noxious substances, such as venoms (Mukai et al., 2016; Palm et al., 2012; Profet, 1991). Beside venoms of insects, arachnids or reptiles, other widespread sources of toxins are bacteria (Rudkin et al., 2017). *Staphylococcus aureus* (SA), a particularly prominent toxin-producing pathogen, can express dozens of toxic molecules, including pore-forming, proteolytic, and exfoliative toxins, as well as superantigenic virulence effectors (Otto, 2014). Also, SA infection is associated with the development of toxin-specific IgE (Kim et al., 2019). This SA infection-associated IgE production has been investigated mostly in the context of exacerbations of allergic disease and experimental evidence suggests significant contributions of SA-derived compounds to the development of atopic dermatitis (Nakamura et al., 2013) and asthma (Stentzel et al., 2017).

It is known that MCs can respond directly to microbial compounds via Toll like- and G-protein-coupled receptors (Arifuzzaman et al., 2019; Pundir et al., 2019; Redegeld et al., 2018), thereby contributing to *innate* host defense against several bacterial species (Arifuzzaman et al., 2019; Piliponsky and Romani, 2018; Pundir et al., 2019). However, the function of MCs as IgE-primed effector cells of *adaptive* immunity is not fully understood (Mukai et al., 2016). We speculated that the MC's antibacterial potential might be substantially increased by IgEs directed against bacterial components. We therefore hypothesized that the type 2 immunity and IgE production observed during bacterial infections might actually be beneficial, at least under certain circumstances, and that this

allergy branch of the antibacterial immune response could represent an important component of adaptive host defense. We here set out to investigate this idea.

Results

Skin-initiated immunity increases systemic host defense against severe SA infection

Epithelial cells are critical for the induction of type 2 immunity and IgE production (Hammad and Lambrecht, 2015; Kobayashi et al., 2019). We therefore applied an epicutaneous SA skin infection model (Nakamura et al., 2013) to trigger a skin-initiated and orchestrated immune response (Figure 1A and S1A). After seven days, infection was associated with increased expression of proinflammatory cytokines and chemokines including type 1 (*Il1b*), type 2 (*Il4*) and type 3 (*Il17a*) immune mediators (Figure S1B), as well as MC degranulation and leukocyte infiltration (Figure S1C and D). Moreover, $CD4^+$ and $CD8^+$ T cells from draining inguinal lymph nodes (ILNs) of infected mice showed increased proliferation upon exposure to toxin-containing, cell-free SA culture supernatant (SA-SN) (Figure S1E). ILN cells of infected mice produced elevated amounts of type 1-3 cytokines (i.e., IFNγ, IL-13 and IL-17a) and IL-2, -6 and -10, but slightly reduced TNF (Figure S1F). Epicutaneous SA infection was also associated with the expansion of ILN T follicular helper (Tfh) cells and the IL-13 producing Tfh (Tfh13) cell subset (Figure S1G and H), which have been assigned critical functions in the production of high-affinity IgE antibodies (Gowthaman et al., 2019).

After 3 weeks of infection, the cutaneous inflammation was associated with increased SA-specific serum IgG1, total IgE (Figure 1B) and SA-specific IgE (Figure 1C). This serum IgE substantially increased degranulation of mouse fetal skin-derived cultured mast cells (FSCMCs) upon SA-SN exposure (Figure 1D), proving its specificity and functionality. In addition, four weeks after epicutaneous back-skin SA (or mock infection), we challenged mice with SA ear skin and soft tissue (ESST) infection (Prabhakara et al., 2013) and found significantly fewer bacteria in both the infected ear (Figure 1E) and the draining (cervical) lymph nodes (Figure 1F) of the mice previously exposed to SA, the latter probably reflecting decreased SA invasiveness (Hahn and Sohnle, 2013; Miller and Simon, 2018). There was also diminished progression of infection, reflected by reduced loss of ear tissue (Figure 1G). This secondary infection increased amounts of specific serum IgG1, IgG2b, and IgG2c, whereas amounts of IgE were not increased significantly compared to those measured after primary infection (Figure 1H and I).

These results indicate that skin-initiated immunity can improve systemic host defense against subsequent SA infection in an organ distant from the original site of pathogen invasion. To further substantiate the systemic effects of skin-initiated immunity, we induced SA pneumonia three weeks after epicutaneous skin infection (Figure 2A). This revealed an earlier induction of antibacterial immune mechanisms in mice with prior SA skin exposure. Specifically, mice which had been exposed to cutaneous SA exhibited elevated amounts of pulmonary IL-1ß and TNF (Figure 2B) and an augmented influx of neutrophils and monocytes (Figure 2C and Figure S2) 6 hours after a second SA challenge. Importantly, this earlier induction of SA-induced inflammation in mice with prior epicutaneous SA infection resulted in an improved bacterial clearance at 18 hours after infection (Figure 2F). It also

was associated with an earlier resolution of inflammation, which was illustrated by both declining amounts of inflammatory cytokines (Figure 2D) and a faster recovery of body temperature (Figure 2E). Finally, mice with prior SA back skin infection that exhibited improved bacterial clearance and recovery after SA pneumonia also had a significant survival advantage (Figure 2G).

Acquired immunity against SA requires IgE effector mechanisms

Having shown that SA skin infection resulted in increased amounts of IgG and IgE, improved host defense against severe SA infection of distant organs, and enhanced survival, we next tested the importance of specific humoral immune effector mechanisms. FcεRIγ-deficient (*Fcer1g*$^{-/-}$) mice lack the common γ-chain required for signaling of several activating (IgG and IgE) Fc receptors (Bruhns and Jonsson, 2015). Notably, skin infection of FcεRIγ-deficient mice induced similar IgG1 and even higher amounts of IgE compared to controls (Figure S3A and B). However, the FcεRIγ-deficient mice did not express any beneficial effect of prior back-skin infection on defense against ESST infection (Figure 3A, B and C).

We next investigated the role of type 2 immunity- and allergy-related effector mechanisms, using mice that lack IgE or FcεRIα (the IgE-binding component of FcεRI). Both IgE-deficient (*Igh-7*$^{-/-}$; Figure 3D and E) and FcεRIα-deficient (*Fcer1a*$^{-/-}$; Figure 3F–H) animals were unable to mount protective immunity against ESST infection despite otherwise developing the expected humoral immune responses (except for lack of IgE in the *Igh-7*$^{-/-}$ mice) upon primary infection (Figure S3C and S3D). Histological analysis of ear MC degranulation 6 hours after ESST infection revealed increased numbers of extensively-degranulated MCs in wild type mice with prior epicutaneous infection, but not in mice lacking functional FcεRI (Figure 3I). Similar to our observations in animals challenged with ESST infection, skin-mediated immunity didn't improve host defense during pneumonia (Figure 4A) in IgE- (Figure 4B and C) or FcεRIα- (Figure 4D and E) deficient mice.

MCs play a critical role in IgE-mediated host defense against SA

IgEs mediate their effector function by antigen-specific priming and activation of immune cells, primarily tetrameric FcεRI-expressing (Balbino et al., 2018) MCs and basophils (Voehringer, 2013). We therefore explored the contributions of these cell populations using cell-deleter models. Diphtheria toxin A (DTA) expression driven by cell type-specific Cre recombinase was employed to delete basophils (*Mcpt8-cre*) or mast cells (*Mcpt5-cre*) (Figure 5A). SA skin exposure in mice that lacked basophils (*Mcpt8-cre; DTA*^{fl}) induced humoral immunity (Figure S4A, B) and increased resistance to ESST infection to a similar extent as in basophil-sufficient (*Mcpt8-cre; DTA*$^{+}$) mice (Figure 5B and C). In contrast, although the IgE and IgG1 response following SA skin exposure in the absence of Mcpt5-expressing MCs (*Mcpt5-cre; DTA*^{fl}) was unaltered (Figure S4C), these mice failed to exhibit the protective antibacterial response upon ESST infection (Figure 5D–F) or pneumonia (Figure 5G–I). We concluded that the SA skin-infection-triggered IgE effector mechanisms enabled MCs to exert protective, antibacterial effects during secondary, distant site infections.

Pore-forming *S. aureus* toxins contribute to increased amounts of IgE

While MCs have been identified as being important during SA-associated atopic dermatitis in mice (Nakamura et al., 2013), they seem to be dispensable for IgE induction in our model (Figure S4C). We hypothesized that tissue damage mediated by cytolytic SA toxins might be an important driver of type 2 immunity and IgE induction (Gause et al., 2020). We tested this idea using a SA strain deficient in five cytolytic toxins (α hemolysin, γ hemolysin, Panton-Valentine leukocidin, leukocidin ED and leukocidin GH) (*S. aureus*^{5xKO}) (Otto, 2014; Rouha et al., 2018). Epicutaneous infection with this strain (Figure S4D) was associated with less-severe skin lesions 7 days after infection, despite comparable epicutaneous bacterial load as compared to wild type bacteria (*S. aureus*^{WT}) (Figure S4E–F), and also led to significantly lower amounts of IgE 14 days later (Figure S4G), suggesting a role for these toxins in IgE induction.

Local allergic reactions and IgE-activated MCs possess antibacterial activity

Having experimental evidence for the potential of bacteria-induced IgEs, and MCs, in orchestrating antibacterial host defense, we also tested whether a well-studied IgE- and MC-mediated allergic reaction to an unrelated antigen might be able to influence resistance against SA. To do this, we combined a mouse model of passive cutaneous anaphylaxis (PCA) to dinitrophenyl (DNP) (Marichal et al., 2013) with local SA infection (Figure 5J). Mice were first intradermally injected with anti-DNP IgE (or vehicle) in the ear and challenged the next day by intravenous injection of DNP-coupled human serum albumin (DNP-HSA), leading to a locally-restricted, mast cell-mediated allergic reaction and ear swelling (Figure 5K). When we combined application of DNP-HSA with simultaneous ESST infection, we observed that IgE-mediated mast cell activation with DNP-HSA markedly increased resistance against SA, reflected by reduced bacterial loads in the ear and draining lymph nodes (Figure 5L and M). This result illustrates the powerful intrinsic antibacterial potential of allergic reactions.

In vivo, the IgE-mediated stimulation of MCs could increase their direct (e.g. by release of bactericidal compounds) and/or indirect (e.g. by release of chemotactic mediators to recruit neutrophils) antibacterial activity (Piliponsky and Romani, 2018). Pre-sensitization of FSCMCs with serum of SA-infected mice enhanced the cells' proinflammatory cytokine production (Figure 6A) and SA killing activity (Figure 6B). Previous studies from our lab (Akahoshi et al., 2011; Metz et al., 2006) and others (Anderson et al., 2018; Schneider et al., 2007) revealed that MCs can contribute to innate host defense by neutralizing toxic venom components. Therefore, we next tested whether mediators released by (anti-DNP) IgE- and antigen (DNP-HSA)-activated FSCMCs can influence the cytotoxic effects of SA-SN on A549 human lung epithelial cells (Figure S5A). Pre-incubation of SA-SN with supernatant of FSCMCs stimulated for 1 h or 20 h by IgE and antigen led to significantly increased viability of A549 cells subsequently exposed to the SA-SN (Figure 6C). To identify the antibacterial effects of released mast cell mediators, we collected supernatants at different times from stimulated FSCMCs and transferred them to SA cultures. Notably, we found that compounds released by FSCMCs within an hour after IgE- and antigen-mediated activation substantially reduced SA viability (Figure 6D).

We then examined the early (1 h) IgE- and antigen-triggered MC secretome by mass spectrometry (MS)-based proteomics. Supernatants of IgE- and antigen-activated FSCMCs (as compared to non-sensitized cells) contained 286 increased proteins (Figure 6E and Figure S5B–S5D) among which five GO (Gene Ontology) molecular function groups were significantly enriched (Figure 6F and Table S1).

Among other top hits were cytokines (e.g., TNF), as well as a series of carbohydrate-modifying and proteolytic enzymes, including mast cell-specific proteases, cathepsins and granzyme B (Figure 6E, Figure S5C and Table S1). As the antibacterial potential of non-MC serine proteases has been previously reported (Stapels et al., 2015; Walch et al., 2014), we hypothesized that the accumulated proteolytic activity of released MC compounds might contribute to their antimicrobial potential. Indeed, we observed that protease inhibitor pre-treatment significantly decreased the antibacterial activity of MC supernatants (Figure 6G) without directly affecting SA growth (Figure S5E). These results indicate that IgE and antigen-activated MCs can rapidly release antibacterial compounds which interfere with SA toxicity and, at least partly by proteolytic activity, with SA growth.

Taken together, these findings illustrate that IgE-mediated activation increases indirect and direct MC activity against SA, by enhancing cytokine production, detoxification, and release of anti-bacterial compounds. We think that, in concert, these mechanisms increase resistance and hasten and enhance the recovery, and the survival, of SA-infected mice.

Discussion

Adaptive type 1 and 3 immune responses are generally considered protective during bacterial infections; by contrast, type 2 immunity is typically regarded as a mal-directed and detrimental response that can drive allergic sensitization and related pathologies (Eberl, 2016). Indeed, IgE and MCs together constitute a central effector module of type 2 immunity that is infamous for its critical role in allergic diseases. However, one possible explanation for the evolutionary conservation of this *allergy module* (IgEs and mast cells) is the *toxin hypothesis*, which suggests that allergic immune responses represent a protective adaptive mechanism against noxious substances (Palm et al., 2012; Profet, 1991).

In fact, while increased serum IgE is a major hallmark of allergies (Galli and Tsai, 2012), human studies show that healthy individuals also can exhibit detectable amounts of IgE specific for toxins of hymenoptera (Langen et al., 2013; Stemeseder et al., 2017) and SA (Sintobin et al., 2019; Van Zele et al., 2004) *without* diagnosed atopic diseases. This might indicate that, at least in some subjects, anti-toxin IgEs are not harmful but instead are beneficial, and that the underlying type 2 immunity is elicited to combat noxious substances or their sources, such as bacteria. In fact, many mediators with direct and/or indirect effects on antibacterial activity can be released by antigen-stimulated IgE-sensitized MCs (Piliponsky and Romani, 2018).

Using SA as a prototypic, toxin-producing bacterium known to induce IgE-associated immune responses, we here tested whether the protective role of the *allergy module* against toxins extends from insects (Marichal et al., 2013; Palm et al., 2013) and reptiles (Starkl et

al., 2016) to a pathogenic bacterium. We found that the epicutaneous infection of mice with SA initiated a mixed adaptive immune response associated with expansion of Tfh13 cells and substantial production of IgE. Notably, the development of IgE in our model required neither basophils nor MCs, which have been shown to contribute to antigen-specific IgE development during a different mouse model of SA-mediated atopic dermatitis (Nakamura et al., 2013). However, we found that amounts of IgE were decreased upon infection with a SA-strain deficient in multiple cytoloytic toxins, suggesting an important role for toxin-mediated tissue damage in promotion of IgE production. It is known that skin tissue injury efficiently induces production of potent type 2 immunity initiating and promoting alarmin cytokines, such as IL-33, TSLP and IL-25 (Kobayashi et al., 2019), possibly contributing to the efficient induction of immunity via this route. We found that the skin-initiated immune response was associated with significantly increased resistance in models of SA infections of the skin and soft tissue, and of the lungs, types of severe SA infections commonly found in humans (Musher and Thorner, 2014; Stryjewski and Chambers, 2008; Torres and Rello, 2010).

We next used genetically-modified mice to decipher the functions of IgE and FcεRI in acquired resistance against SA. We observed that immunized IgE-deficient or FcεRIα-deficient (Figure 4D) mice showed significantly lower body temperature (18 hours after infection) compared to the respective PBS mock-immunized genetically ablated animals. This finding resembles previous results in honeybee venom-immunized IgE-deficient (Marichal et al., 2013) and Russell's viper venom immunized FcεRIα-deficient (Starkl et al., 2016) mice after their challenge with a high dose of the respective venom. These results may indicate that protective adaptive immune responses against various toxins could become detrimental, for instance due to IgG-mediated systemic anaphylaxis, if IgE is absent or can't activate FcεRIα-bearing effector cells.

IgE bound to FcεRI can increase MC responsiveness to minute amounts of antigen (Galli and Tsai, 2012), resulting in the rapid release of cytoplasmic granules containing proteoglycans, vasoactive amines, proteases, and certain cytokines, as well as anti-microbial peptides (Wernersson and Pejler, 2014). In addition, following degranulation, MCs synthesize and release many lipid mediators, cytokines and chemokines (Mukai et al., 2018). While MCs could be directly activated by microbial compounds (Nakamura et al., 2013; Pundir et al., 2019; Redegeld et al., 2018), we here found that IgE-containing immune serum could profoundly increase MC responsiveness and antibacterial activity. Taken together, our results provide evidence for a previously unappreciated function of type 2 immunity, IgEs and MCs: promoting increased *adaptive* host defense against bacteria.

Infection with SA, and the rise of antibiotic-resistant strains, are serious worldwide health problems responsible for many deaths (Cassini et al., 2019). Considering the importance of IgE and MCs in our experimental setting, it appears possible that approaches for treating atopic diseases with compounds that interfere with IgE and type 2 cytokine activity (Cosmi et al., 2019) might also impair immune responses against pathogenic bacteria. Although our study illustrates the potential of type 2 immunity and IgE-activated MCs for promoting host defense against SA in mice, the *allergy module* can also elicit life-threatening situations if

unleashed systemically (Galli and Tsai, 2012; Reber et al., 2017). Caution therefore will be required to assess any potential exploitation of the *allergy module* in therapeutic approaches.

STAR Methods

Resource availability

Materials availability statement—Further information and requests for resources and reagents should be directed to and will be fulfilled by the Lead Contact, Philipp Starkl (philipp.starkl@meduniwien.ac.at).

Data and code availability statement—The mass spectrometry proteomics data have been deposited to the ProteomXchange Consortium via the PRIDE (Perez-Riverol et al., 2019) partner repository with the dataset identifier PXD019107 and 10.6019/PXD019107.

Additional resources—Not applicable

Experimental model and subject details

Mice—All animal experiments were carried out in accordance with current guidelines of the National Institutes of Health and US and Austrian law after approval by the Institutional Review Boards of Stanford University (IACUC; protocol ID 29820) and the Medical University of Vienna and the Austrian Ministry of Sciences (protocol ID BMWF-66.009/0149-WF/V/3b/2015). Healthy age-matched 8-10 week old female mice were used throughout the study. Mice were housed at the Dept. for Biomedical Research of the Medical University of Vienna, the Institute for Molecular Biotechnology (IMBA), Vienna, Austria, and at Stanford University, Stanford, CA, USA. C57BL/6J mice were maintained in local mouse facilities. In experiments with Cre-mediated deleter mice (*Mcpt5-cre; Mcpt8-cre;*), littermate controls (*Mcpt5*-WT*; DTA*^{fl} or *Mcpt8-cre; DTA*$^{+}$, respectively) were used. In experiments with full body gene deficiency mice (*Fcer1g*$^{-/-}$*, Igh-7*$^{-/-}$*, Fcer1a*$^{-/-}$), mice (already on the C57BL/6J background as described below) were back-crossed (one time) to locally maintained C57BL/6J mice. Resulting heterozygous F1 mice were then bred to generate homozygous breeders which were used to generate $^{+/+}$ and $^{-/-}$ mice used in experiments. Mcpt5-cre$^{(Tg(Cma1-cre)Aroer}$ (Scholten et al., 2008)) were generously provided by Axel Roers (Technical University Dresden, Germany). *Mcpt8-cre* (B6.129S4-*Mcpt8*$^{tm1(cre)Lky}$/J (Sullivan et al., 2011)), *DTA*^{fl} (B6.129P2-*Gt(ROSA)26*$^{Sortm1(DTA)Lky}$/J (Voehringer et al., 2008)) and *Fcer1a*$^{-/-}$ mice on C57BL/6J background (B6.129S2(Cg)-*Fcer1a*^{tm1Knt}/J (Dombrowicz et al., 1993)) were originally obtained from Jackson Laboratories. *Fcer1g*$^{-/-}$ (B6.129P2-*Fcer1g*^{tm1Rav} N12 (Takai et al., 1994), backcrossed 12 generations to C57BL/6J) were originally obtained from Taconic. *Igh-7*$^{-/-}$ (*Igh-7*^{tm1Led} (Oettgen et al., 1994)) mice were generously provided by Hans C. Oettgen (Harvard Medical School, Boston, MA, USA) and obtained backcrossed for 8 generations on the C57BL/6J background from Mitchell Grayson (Medical College of Wisconsin, Milwaukee, WI, USA).

Bacterial strains and culture—The wild type methicillin-resistant *Staphylococcus aureus* strain USA300 LAC (Diep et al., 2006; Popov et al., 2015) was kindly provided by Fabio Bagnoli (GSK Vaccines, Siena, Italy). *S. aureus* lacking five pore-forming toxins (*S.*

aureus^{5xKO}): α hemolysin (*hla*), γ hemolysin (*hlgACB*), Panton-Valentine leucocidin (*lukSF-PV*), leukocidin ED (*lukED*) and leukocidin GH (*lukGH* also known as *lukAB*) and the respective isogenic USA300 WT strain (*S. aureus*^{WT}; ATCC BAA-1717) (Badarau et al., 2016; Rouha et al., 2018) were provided by Lukas Stulik. For bacterial culture, frozen stocks were streaked on tryptic soy agar plates and grown overnight at 37°C. A single colony was picked to inoculate 10 ml tryptic soy broth (TSB) and grown overnight at 37°C with shaking at 180 rpm. The overnight culture was used to inoculate fresh room-temperature tryptic soy broth in an Erlenmeyer flask at a dilution of 1:200. Bacteria for infections (see below) were harvested, after (typically 2-3 h) culture at 37°C, at 180 rpm at an OD_{600} of 0.5 – 0.9 by centrifugation for 5 min at 1800 g at 4°C and washed once with endotoxin-free PBS. Before infections, serial dilutions of the inoculum were plated on tryptic soy agar in order to quantify the titer (viable bacteria). For quantification of tissue bacterial loads, serial dilutions of tissue homogenates were plated on Baird-Parker agar. CFUs indicated in the graphs are per ml tissue homogenate.

For generation of the cell-free *S. aureus* culture supernatant (SA-SN) that was used for IgG ELISAs and MC stimulation experiments, overnight bacterial culture was diluted 1:200 in fresh tryptic soy broth in an Erlenmeyer flask and incubated for 16 hours shaking at 180 rpm at 37°C. Bacterial suspensions were centrifuged 5 min at 1800 g at 4°C. Supernatant was then transferred to a fresh tube, centrifuged one more time and subsequently filtered using a Stericup-GV (0.22 μm pore size) filter unit (Millipore). Cell free, filtered supernatant was next concentrated 20x by centrifugation at 4°C using Pierce Protein Concentrators (3K MWCO; Thermo Fisher Scientific). Concentrated supernatant was next 2x dialyzed overnight at 4°C using Pierce SnakeSkin Dialysis Tubing (3500 MWCO; Thermo Fisher Scientific) against 1 L PBS/ml supernatant. Concentrated and dialyzed SA-SN (or equally processed, plain TSB as control for activation experiments) was aliquoted and stored at −80°C.

For generation of SA-SN used for specific IgE ELISAs and detoxification experiments, overnight bacterial cultures were diluted 1:200 in fresh sterile-filtered RPMI without phenol red (Gibco) supplemented with 1% casamino acids (VWR) and incubated for at 37°C for 16 hours with shaking at 180 rpm. Bacterial suspensions were centrifuged for 5 min at 1800 g at 4°C. Supernatants (or RPMI 1% casamino acids) were then processed as above, to obtain 20x concentrated supernatants, and stored at −80°C.

Bacterial infection models

Epicutaneous back skin *S. aureus* infection: For the epicutaneous back skin *S. aureus* infection model (Nakamura et al., 2013), centrifuged bacteria (see above) were resuspended at 10^9 CFUs/ml in endotoxin-free PBS and kept on ice. Anesthetized mice were shaved on the torso between fore- and hind legs using a clipper (Oster). Hair loosely attached on the back was removed using a piece of paper tape. Mice were then tape-stripped 5 times on the back using 3-4 cm pieces of tape. Afterwards, we applied an approximately 1.0 x 1.5 cm piece of gauze inoculated with 100 μl bacterial suspension (containing 10^8 CFUs) or PBS (mock infection). The patch was then fixed in place using Tegaderm Transparent Film Roll (3M). After one week, mice were anesthetized again and the patch was removed. Bacterial

load on day 7 was estimated by epicutaneous sampling using skin swabs (pre-wet in sterile PBS) which were then incubated in PBS for 20 minutes on ice in microcentrifuge tubes containing 500 μl PBS. After removing the swabs, the bacteria were pelleted by centrifugation for 10 minutes at 1800 g, resuspended in 100 μl, serially diluted in 1:10 steps and plated in 10 μl drop triplicates on Baird-Parker agar plates for overnight incubation at 37°C and quantification (Popov et al., 2015).

To assess the importance of selected SA toxins for IgE production, mice were epicutaneously infected with a mutant strain (*S. aureus*^{5xKO}) lacking five pore-forming toxins α hemolysin (*hla*), γ hemolysin (*hlgABC*), Panton-Valentine leukocidin (*lukSF-PV*), leukocidin ED (*lukED*) and leukocidin GH (*lukGH* also known as *lukAB*) or with the respective isogenic USA300 WT strain (*S. aureus*^{WT}; strain designation TCH1516; ATCC BAA-1717) (Badarau et al., 2016; Rouha et al., 2018).

***S. aureus* ear skin and soft tissue (ESST) infection:** For ESST infection (Popov et al., 2015; Prabhakara et al., 2013), centrifuged bacteria (see above) were resuspended at 10^{11} CFUs/ml in endotoxin-free PBS and kept on ice. Mice were anesthetized and the left ear was thoroughly cleaned with 70% isopropanol and allowed to dry. Ten μl of the inoculum (10^9 CFUs) were dispensed onto the tip of a sterile Morrow Brown allergy-testing plastic needle (Morrow Brown Allergy Diagnostics). The cleaned ear was then pricked 10 times with the SA-coated needle. For endpoint experiments 20 hours after infection, the infected ear was cleaned thoroughly (superficially) with 70% isopropanol and collected along with cervical lymph nodes and homogenized for quantification of bacteria.

***S. aureus* pneumonia:** For induction of pneumonia (Inoshima et al., 2011; Popov et al., 2015), centrifuged bacteria (see above) were resuspended in endotoxin-free PBS at a density of approximately 10^{10} CFUs/ml (for experiments performed at Stanford University) or approximately 2x 10^9 CFUs/ml (for experiments performed at the Medical University of Vienna) – the different inoculates of bacteria used were applied due to differing susceptibilities of wildtype mice in pilot experiments (data not shown), which might be explained by differences in housing conditions or microbiome composition. Anesthetized mice were intranasally inoculated with 30 μl in the left nostril (to achieve inoculates of approximately 3x 10^8 or 6x 10^7 CFUs/mouse, respectively). Body temperature was measured using a rectal thermometer.

Tissues for bacterial quantification, RNA and protein analysis were homogenized using the Precellys system (Bertin Instruments).

IgE-dependent passive cutaneous anaphylaxis combined with ESST infection: Mice were sensitized in both ears with one intradermal injection per ear of 20 μl PBS containing 20 ng anti-dinitrophenyl (DNP) IgE (kindly provided by Dr. Fu-Tong Liu, then at University of California-Davis, Davis, Ca) (Liu et al., 1980) to sensitize mast cells, or received PBS only (using a 30 g needle on a one ml syringe; BD Biosciences) into both ears (Marichal et al., 2013). 18 hours later, the mice were anesthetized and treated with the ear skin and soft tissue (ESST) infection model. Immediately after ear pricking, 100 μl of 0.9% saline containing 100 μg DNP_{30-40}-conjugated human serum albumin (DNP-HSA; Sigma) was

injected into the retro-orbital vein to induce mast cell degranulation in IgE-sensitized ears. Thickness of the non-infected ear was measured using a dial thickness gauge (model G-1A; Peacock Ozaki) in order to assess degranulation-mediated ear swelling. Ears and cervical lymph nodes were harvested after 20 hours as described above.

Fetal skin-derived cultured mast cells (FSCMCs)—FSCMCs were generated based on a published protocol with some modifications (Meindl et al., 2006). Pregnant mice were euthanized on day 17 or 18 of pregnancy. Twenty minutes later, the peritoneum was opened and the uterus containing the fetuses was excised and transferred into a 50 ml tube containing sterile endotoxin-free PBS and kept on ice. Under a sterile lamina flow hood, the fetuses were dissected from the uterus and washed 2 times by floating in two dishes with sterile endotoxin-free PBS. Fetuses were then transferred into 12 well plates (one fetus per well) containing 2 ml 0.05% Trypsin EDTA with phenol red (Gibco, Thermo Fisher Scientific) 100 u/ml DNase (Sigma). Plates were incubated at 37°C in an incubator for a total of 30 minutes. Every 5 minutes, plates were gently swirled and after 15 minutes, fetuses were laterally reversed. After incubation, remainders were removed and the cell suspension was pooled and filtered over a 70 μm cell strainer (BD Biosciences) and RPMI 10% FBS was added over the strainer to stop the digest. Cells were then centrifuged and resuspended in RPMI 10% FBS 10 mM HEPES, 1x nonessential amino acids, 1 mM sodium pyruvate, 50 μM ß-mercaptoethanol (all media and supplements from Gibco apart from FBS, which was obtained from Sigma), supplemented with 10 ng/ml IL-3 and 10 ng/ml SCF (both from Peprotech). Cell fractions equivalent to 3 fetuses were seeded in 100 ml medium in 175 cm^2 tissue culture flasks and cultured for 4 weeks without medium change. After 4 weeks, cells were harvested by centrifugation and seeded in 50 ml fresh medium for 2 additional weeks before assessment of maturation by flow cytometry and degranulation capacity. After 6 weeks, typically more than 95% of the cells were FcεRIα/c-Kit double positive and could be activated efficiently with IgE and antigen. Cells were used between 6 – 12 weeks of age.

Method details

Flow cytometry—For flow cytometry analysis, the entire right and left lungs were harvested and weighed. Representative pieces of each lobe were pooled, weighed and cut into small pieces in 250 μl RPMI medium containing 5% fetal calf serum (FCS) in an Eppendorf tube. Lung pieces were then transferred to a 6 well plate and 3 ml of digestion medium (RPMI 5% FCS containing 250 U/ml Collagenase I (Gibco) and 20 U/ml DNAse I (Sigma)) were added to each well, followed by 45 minutes incubation at 37°C shaking at 100 rpm. Digested samples were then homogenized 15 times in a Dounce tissue homogenizer (VWR) and filtered over a 70 μm cell strainer (BD Biosciences). After centrifugation (5 minutes at 300 g, 4°C), the pellet was treated for 5 minutes with ACK buffer (150 mM NH_4Cl, 10 mM $KHCO_3$, 0.1 mM Na_2EDTA, pH 7.2 – 7.4) for erythrocyte lysis. After stopping erythrocyte lysis by addition of PBS 1% bovine serum albumin (BSA; Sigma), cells were filtered over a 40 μm cell strainer (BD Biosciences), centrifuged, resuspended and counted. Single cell suspensions were treated with TruStain fcX (anti-mouse CD16/32; BioLegend) and Fixable Viability Dye eFluor 780 (eBioscience) according to the manufacturer's instructions. Subsequently, fluorescently-labelled antibodies were added and stained for 20 minutes on ice. Cells were then washed and fixed for 30 minutes at

room temperature using the Fixation Medium of the Fix and Perm Cell Fixation and Permeabilization Kit (Nordic MUbio). Stained and fixed cell suspension was analyzed using an LSRFortessa (BD Biosciences). Data were analyzed using FlowJo software (FlowJo LLC) up to version 10.5.0. The fluorescently-labelled anti-mouse antibodies (all obtained from BioLegend unless specifically indicated) as listed in the key resources table were used throughout this study.

Analysis of T cell responses—Antigen-specific proliferation of inguinal lymph node cells was analyzed as previously described (Marichal et al., 2013). Briefly, inguinal lymph nodes (ILNs) were harvested from infected mice 7 days after infection. Lymph nodes were minced on a 70 μm cell strainer into PBS (BD Falcon). After rinsing the strainer with PBS, cells were centrifuged, resuspended in pre-warmed PBS and counted. 1/10 volume of 50 μM CellTrace CFSE (Invitrogen) in PBS was added to cells adjusted to 5.5x 10^7 cells/ml. Staining was performed for 8 minutes in a 37°C water bath protected from light with brief vortexing every two minutes. Ice-cold RPMI supplemented with 10% FBS and 1% penicillin/streptomycin (complete RPMI) was added to stop the reaction before incubation on ice for 5 min. Stained cells were washed and resuspended at 3x 10^6 cells/ml in complete RPMI and seeded at 100 μl in 96 well round bottom plates (Costar). 100 μl of 2x stimulants (concentrated SA-SN or TSB was pre-diluted 1:1 to finally yield a final 5x concentration). After incubation for 96 hours at 37°C, cells were centrifuged and cell supernatant cytokines were analyzed using a cytometric bead array (BD Biosciences). Cells were stained for flow cytometry, fixed and analyzed using an LSRII flow cytometer (BD Biosciences). Percentages of CFSE-low (proliferated) among $CD45^+$ $CD4^+$ $CD8^-$ T_{Helper} and $CD45^+$ $CD8^+$ $CD4^-$ cytotoxic T cells are reported.

The T follicular helper (T_{FH}) cell response was analyzed in ILNs harvested from mice 7 days after infection. Cell suspensions were prepared from lymph nodes as described above. ILN cells were seeded in 100 μl IMDM medium (Gibco) supplemented with 10% FCS and 1% penicillin/streptomycin (complete IMDM) in a 96 well round bottom plate and stimulated by addition of 100 μl complete IMDM containing 100 ng/ml phorbol 12-myristate 13-acetate (PMA, Sigma) and 2 μg/ml ionomycin for 1 hour in a tissue culture incubator at 37°C. After addition of 20 μl GolgiStop (1:150 pre-diluted; BD Biosciences), cells were incubated for 3 more hours. Extracellular and intracellular staining was performed as previously described (Gowthaman et al., 2019). Briefly, cells were washed and stained 30 minutes at 4°C with surface staining antibodies, followed by fixation (20 minutes at 4°C) and permeabilization (15 minutes at 4°C after 2 prior washes in Perm/Wash solution) using the Fixation/Permeabilization Solution Kit (BD Biosciences). Intracellular cytokines were stained in Perm/Wash solution containing anti-cytokine antibodies overnight at 4°C. After 2 washes with Perm/Wash solution, cells were resuspended in PBS and analyzed using an LSRFortessa.

Histology—Tissue samples were fixed in 7.5% formalin, embedded in paraffin, cut into 5 μm thick sections, followed by staining with Hematoxylin & Eosin or Toluidine Blue. Whole sections were recorded using a Vectra Plaris microscope (PerkinElmer) at the Imaging Core Facility of the Medical University of Vienna. Mast cell degranulation on whole tissue

sections was assessed by a blinded experimenter using QuPath software version 0.2.0 (Bankhead et al., 2017) and is expressed as % of at least 70 examinded skin MCs/section: “Extensive” refers to >50%, “Moderate” to 10-50% and “None” to <10% of cytoplasmic granules of a MC exhibiting alterations in staining characteristics, granule size or distribution (regarded as morphological evidence of degranulation) (Marichal et al., 2013).

Mast cell degranulation and S. aureus co-culture experiments—For assessment of serum IgE functionality and specificity, 3x 10^5 FSCMCs were sensitized in 300 µl medium in a 48 well plate by overnight incubation with 30 µl of serum collected from wild type mice 21 days after epicutaneous skin infection with SA or PBS. In order to block binding of IgE to FcεRI, serum from SA-infected mice was pre-treated by incubation with 5 µg anti-mouse IgE (clone R35-92; BD Pharmingen) (or mock-treated with rat IgG1 isotype [clone R3-34; BD Pharmingen]) for 30 minutes at room temperature (Marichal et al., 2013). The next day, cells were collected, centrifuged, washed once with Tyrode’s buffer (100 mM HEPES, 130 mM NaCl, 1.8 mM $CaCl_2$, 5 mM KCl, 2 mM $MgCl_2$, 5.5 mM glucose, 1 g/L bovine serum albumin (BSA); pH 7.4; all reagents were obtained from Sigma) and stimulated in quadruplicates with a final 1:50 diluted *S. aureus* culture supernatant (SA-SN) or tryptic soy broth (TSB) (see above; this dilution is equivalent to 0.5x concentrated culture supernatant or plain medium) in Tyrode’s buffer for 60 minutes at 37°C. As an indicator of degranulation, release of ß-hexosaminidase into the supernatant (as percentage of the combined signal of supernatant and cell lysate) was measured using the chromogenic substrate 4 mM p-nitrophenyl-N-acetylß-D-glucosaminide (Sigma) as previously described (Akahoshi et al., 2011).

For analysis of direct antimicrobial effects of mast cells against SA (Figure 6B), FSCMCs were sensitized with serum as described above. The next day, cells were collected and washed with DMEM (Gibco) 10% FBS (without antibiotics) and resuspended at 5x 10^6 cells/ml (equivalent to 10^5 cells/20 µl) and seeded at 40 µl in quadruplicates in 96 well round bottom plates (Costar). Diluted SA overnight culture (see above) was harvested at OD_{600} 0.5 – 0.9, washed with endotoxin-free PBS and resuspended at 5x 10^6 CFUs/ml DMEM + 10% FBS. Next, 20 µl SA suspension (10^5 CFUs) were added to the cell suspension, followed by 20 µl of DMEM 10% FBS to a total volume of 80 µl. After brief and thorough mixing, suspensions were incubated 6 hours at 37°C (without shaking), followed by thorough resuspension, preparation of serial dilutions, and plating on Baird-Parker agar for determination of viable bacteria.

For generation of mast cell supernatants for SA co-culture experiments (e.g. Figure 6D), FSCMCs were sensitized overnight with 1 µg/ml anti-DNP IgE (or non-sensitized). The next day, cells were centrifuged and washed 2x with DMEM medium without phenol red + 10% FBS without antibiotics and resuspended at 10^7 cells/ml. Three groups of IgE-sensitized and non-sensitized cells were stimulated in triplicate by addition of 1 volume of pre-warmed 2x stimulus (final concentration of 10 ng/ml DNP-HSA) in DMEM 5% FBS and a density of 5x 10^6 cells/ml (equivalent to 10^5 cells/20 µl). From the first group, supernatant was collected after 1 hour and replaced with fresh medium containing 1x stimulus and the stimulation was continued for another 19 hours. From the second group, supernatant was collected after 6 hours and stimulation was continued with fresh medium and stimulus for another 14 hours.

From the third group supernatant was collected after 20 hours, together with the supernatant from groups one and two (which at this point were deficient of mediators produced during the first and first six hours after antigen addition, respectively). Supernatants were stored at −80°C.

For experiments to assess the anti-bacterial activity of mast cell compounds, diluted SA overnight culture (see above) was harvested at OD_{600} 0.5 – 0.9, washed with endotoxin-free PBS and resuspended at 5x 10^6 CFUs/ml DMEM + 10% FBS. Next, 20 μl SA suspension (10^5 CFUs) were added to 40 μl of DMEM 10% FBS in triplicates in 96 well round bottom plates (Costar) and 20 μl of either medium or mast cell supernatant (see above) was added and mixed. After 6 hours of culture at 37°C (without shaking), cultures were thoroughly resuspended and serial dilutions of the suspension were prepared and plated on Baird-Parker agar for determination of viable bacteria. In experiments to investigate the importance of mast cell protease activity, mast cell supernatant was pre-incubated with 8 μl of 20x Complete Mini EDTA free protease inhibitor (Roche) for 10 minutes at room temperature. SA suspension and medium to 80 μl total volume was added as above.

A549 cell viability and detoxification assay—Human lung epithelial A549 cells (ATCC, CCL-185) were cultured in DMEM supplemented with 10% FBS 1% penicillin/streptomycin (complete DMEM). For assessment of SA-SN toxicity, A549 cells were seeded at 4x 10^4 cells/well in 96 well flat bottom plates. On the next day, the medium was replaced with complete DMEM containing different dilutions of 20x concentrated SA-SN (prepared as described above) or RPMI 1% Casaminoacids – the dilutions indicated refer to the actual SA-SN before concentration. After 20 hours incubation, cell viability was assessed using the CellTiter-Glo Lumincescent Cell Viability Assay (Promega) following the manufacturer's instructions.

For testing the detoxifying potential of IgE- and antigen-activated mast cells, supernatants from anti-DNP IgE-sensitized or non-sensitized cells was collected from cells stimulated for 1 or 20 hours with 10 ng/ml DNP-HSA as described above. Twenty times-concentrated SA-SN or RPMI 1% casamino acids was diluted 1:20 in mast cell supernatant and incubated for 1 hour at 37°C. Next, 6.5 reaction volumes of complete DMEM were added and 100 μl of this mix was added to A549 cells (seeded the day before as described above), resulting in a final 1:7.5 dilution of SA-SN (or RPMI 1% casamino acids). Cell viability was assessed after 20 hours incubation.

Analysis of serum IgG and total IgE antibodies—Serum antibodies were analyzed based on previously described protocols (Marichal et al., 2013; Starkl et al., 2016). Briefly, for detection of SA-specific IgG antibodies, MaxiSorp ELISA plates (Nunc) were coated with 50 μl of SA-SN 1:500 diluted in PBS overnight at 4°C, followed by blocking with 200 μl of 1% BSA for at least 2 hours at room temperature. Sera were diluted in PBS 1% BSA at 1:50, 1:200, 1:800 and 1:3200 (for investigation of the primary antibody response at day 21 after epicutaneous skin infection) or 1:800, 1:3200, 1:12800 and 1:51200 (for investigation of the secondary antibody response 14 days after ear skin and soft tissue (ESST) infection) and 50 μl were incubated in the blocked wells for either for 2 hours at 37°C or overnight at 4°C. After three washing steps with PBS containing 0.05 % tween, wells were incubated

with 1:1000 diluted biotinylated rat anti-mouse IgG1 (clone A85-1, BD Pharmingen), rat anti-mouse IgG2b (clone R12-3, BD Pharmingen) or goat anti-mouse IgG2c (polyclonal, Southern Biotech) for 1 hour at room temperature. After washing three times, horseradish peroxidase-conjugated streptavidin (BD Pharmingen) was added for 20 minutes at room temperature, followed by six washing steps and detection using the supersensitive TMB liquid substrate (Sigma). Signal was measured using a Sunrise microplate reader (Tecan) at 450 nm with 620 nm reference. Titers of SA-SN-specific IgG1 were calculated by plotting of the serum dilution that gave half-maximal signal of a reference serum (a pool of sera obtained from infected mice). Total serum IgE was determined in 1:10-diluted sera following a similar protocol as above, using 2 μg/ml rat anti-mouse IgE (clone R35-72, BD Pharmingen) for coating, biotinylated rat anti-mouse IgE (clone R35-118; BD Pharmingen) for detection and serial dilutions of purified mouse IgE (clone C38-2; BD Pharmingen) as standard for quantification of absolute amounts of serum IgE (Marichal et al., 2013; Starkl et al., 2016). Sera and detection reagents were diluted in PBS 1% BSA. All washing steps were performed with PBS containing 0.05% Tween.

Analysis of specific serum IgE antibodies—We developed a capture ELISA assay to detect the presence of SA-SN-specific serum IgE antibodies using biotinylated SA-SN. Four ml of 5x concentrated SA-SN (prepared from bacteria cultured in RPMI 1% casamino acids; see above) was buffer-exchanged to PBS using Zeba Spin-desalting columns (7000 MWCO; Thermo Fisher Scientific; following manufacturer's protocol A) prior to biotinylation with 1 mg EZ-Link Sulfo-NHS-Biotin (Thermo Fisher Scientific) for 2 hours at 4°C and desalting using Zeba Spin-desalting columns (following manufacturer's protocol B). Successful biotinylation was confirmed by Western Blot (data not shown). For SA-SN IgE ELISA, IgE was captured as above in an anti-mouse IgE-coated ELISA plate from 1:1 diluted serum during overnight incubation at 4°C. After washing 3 times (with PBS containing 0.05% Tween), biotinylated SA-SN was added 1:750 diluted in PBS 1% BSA for 3 hours at room temperature. After washing six times, horseradish peroxidase-conjugated streptavidin was added for 20 minutes at room temperature, followed by six washing steps and detection as described above.

Cytokine and chemokine analysis—Tissue cytokines and chemokines were determined using ELISA kits for mouse IL-6 (eBioscience), CXCL-1 (R&D Systems), MIP-2 (R&D Systems). Mediators produced by *ex vivo* stimulated inguinal lymph node cells were determined using a cytometric bead array (BD Biosciences) and a mouse IL-13 ELISA (eBiosciences). Mediators produced by FSCMCs were analyzed using a Procarta Mix&Match 11-Plex assay (Thermo Fisher Scientific) for analysis of GRO-alpha (Cxcl-1), IFNg, IL-1a, IL-1b, IL-10, IL-12p70, IL-4, IL-6, MCP-1, Mip2 and TNF (only data for cytokines that were detected are shown in Figure S1F). All assays were performed following the manufacturer's instructions.

Real-time PCR analysis—Skin samples (approximately 5x 5 mm) from sites in contact with epicutaneous skin patches were snap frozen in liquid nitrogen and ground with (liquid nitrogen-cooled) mortar and pestle. Tissue powder was transferred into 4.5 ml cryogenic tubes (Nunc) and homogenized on ice in 500 μl Trizol (Invitrogen) using an Ultra Turrax

rotor-stator homogenizer (increasing speed over 5 seconds to 20 seconds at full speed). RNA was purified according to the manufacturer's instruction. One μg RNA was transcribed into cDNA using the High-Capacity cDNA Reverse Transcription Kit (Applied Biosystems). Real-time PCR was performed on a StepOnePlus Real-time PCR system (Applied Biosystems) using the Power SYBR Green PCR Master Mix (Applied Biosystems) and the primers as indicated in the key resources table. Relative gene expression fold change was calculated using the ΔΔCt method in relation to the mean of mock (PBS)-infected tissue expression amounts.

Mass spectrometry

LC-MS/MS-based proteomics analysis: For generation of supernatants for analysis by mass spectrometry (MS), FSCMCs were sensitized overnight with 1 μg/ml anti-DNP IgE (or non-sensitized). The next day, cells were washed 2x in DMEM (without supplements) and resuspended at a density of 10^7 cells/ml in DMEM. Cells were then seeded at 50 μl in triplicates in 96 well round bottom plates and pre-warmed 10 minutes at 37°C in an incubator. Next, 50 μl of pre-warmed 20 ng/ml DNP-HSA in DMEM was added and samples were incubated 1 hour at 37°C. Cellular responses were stopped by incubation for 10 minutes on ice. After 5 min centrifugation at 500 g and 4°C, cell-free supernatant was transferred into protein LoBind tubes (Eppendorf), snap-frozen in liquid nitrogen and stored at −80°C until analysis by MS.

Supernatants were processed for LC-MS/MS using an adapted Single-Pot solid-phase-enhanced sample preparation (SP3) methodology published by Hughes *et al.* (Hughes et al., 2014). Briefly, equal volumes (125 μl/6250 μg) of two different kinds of paramagnetic carboxylate-modified particles (SpeedBeads 45152105050250 and 65152105050250, GE Healthcare) were mixed, washed three times with 250 μl water and reconstituted to a final concentration of 50 μg/μl with LC-MS grade water (LiChrosolv, MERCK KgaA, Germany). Supernatants (70 μl) were mixed and normalized to a final volume of 100 μl with 5x sample buffer (10% SDS, 200 mM HEPES, pH 8.0) to a final concentration of 2% SDS, proteins were reduced with a final concentration of 10 mM DTT and incubated at 56°C for 1 hour. After cooling down to room temperature, reduced cysteines were alkylated with iodoacetamide at a final concentration of 55 mM for 30 min in the dark. For tryptic digestion, 400 μg of mixed beads were added to reduced and alkylated samples, vortexed gently and incubated for 5 minutes at room temperature. The formed particles-protein complexes were precipitated by addition of acetonitrile to a final concentration of 70% [V/V], mixed briefly before incubating for 18 minutes at room temperature. Particles were then immobilized using a magnetic rack (DynaMag-2 Magnet, Thermo Fisher Scientific) and supernatant discarded. SDS was removed by washing two times with 200 μl 70% ethanol and one time with 180 μl 100% acetonitrile. After removal of organic solvent, particles were resuspended in 100 μl of 50 mM NH_4HCO_3 and samples digested by incubating with 1 μg of trypsin overnight at 37°C. Peptides were cleaned by acidifying the samples to a final concentration of 1% TFA prior to immobilizing the beads on the magnetic rack to perform solid phase extraction of the recovered supernatant using C18 SPE columns (SUM SS18V, NEST group) according to the manufacturer. Peptides were eluted using two

times 50 µl 90% acetonitrile, 0.4% formic acid, dried in a vacuum concentrator before reconstitution in 26 µl of 5% formic acid (Suprapur, MERCK).

Liquid chromatography mass spectrometry was performed on a Q Exactive Hybrid Quadrupole-Orbitrap (Thermo Fisher Scientific) coupled to a Dionex U3000 RSLC nano system (Thermo Fisher Scientific) via nanoflex source interface. Tryptic peptides were loaded onto a trap column (Acclaim PepMap 100 C18, 3µm, 5 × 0.3 mm, Thermo Fisher Scientific) at a flow rate of 10 µl/min using 5% acetonitrile in 0.1% TFA as loading buffer. After loading, the trap column was switched in-line with a 30 cm, 75 µm inner diameter analytical column (packed in-house with ReproSil-Pur 120 C18-AQ, 3 µm, Dr. Maisch). Mobile-phase A consisted of 0.4% formic acid in water and mobile-phase B of 0.4% formic acid in a mix of 90% acetonitrile and 10% water. The flow rate was set to 230 nl/min and a 90 min gradient used (4 to 24% solvent B within 82 min, 24 to 36% solvent B within 8 min and, 36 to 100% solvent B within 1 min, 100% solvent B for 6 min before re-equilibrating at 4% solvent B for 18 min).

For the MS/MS experiment, the Q Exactive mass spectrometer (Thermo Fisher Scientific) was operated in a top 10 data-dependent acquisition mode with a MS^1 scan range of 375 to 1650 m/z at a resolution of 70000 (at 200 m/z). Automatic gain control (AGC) was set to a target of 1x 10^6 and a maximum injection time of 55 ms. MS^2-scans were acquired at a resolution of 15000 (at 200 m/z) with AGC settings of 1x 10^5 and a maximum injection time of 110 ms. Precursor isolation width was set to 1.6 Da and the HCD normalized collision energy to 28%. The threshold for selecting precursor ions for MS^2 was set to ~2000. Dynamic exclusion for selected ions was 60 s. A single lock mass at m/z 445.120024 was employed (Olsen et al., 2005). All samples were analyzed in duplicate, back-to-back replicates. XCalibur version 4.1.31.9 and Tune 2.9.2926 were used to operate the instrument.

The mass spectrometry proteomics data have been deposited to the ProteomXchange Consortium via the PRIDE (Perez-Riverol et al., 2019) partner repository with the dataset identifier PXD019107 and 10.6019/PXD019107.

Mass spectrometry data analysis: Acquired raw data files were processed using the Proteome Discoverer 2.2.0.388 platform, utilizing the database search engine Sequest HT. Percolator V3.0 was used to remove false positives with a false discovery rate (FDR) of 1% on amounts of peptide and protein under strict conditions. Searches were performed with full tryptic digestion against the human SwissProt database v2017.06 (20456 sequences and appended known contaminants) with up to two miscleavage sites. Oxidation (+15.9949 Da) of methionine was set as a variable modification, whilst carbamidomethylation (+57.0214 Da) of cysteine residues was set as a fixed modification. Data were searched with mass tolerances of ±10 ppm and 0.025 Da on the precursor and fragment ions, respectively. Results were filtered to include peptide spectrum matches (PSMs) with Sequest HT cross-correlation factor (Xcorr) scores of ≥1 and high peptide confidence. For calculation of protein areas Minora Feature Detector node and Precursor Ions Quantifier node, both integrated in Thermo Proteome Discoverer, were used. Automated chromatographic alignment and feature linking mapping were enabled with total peptide amount used for normalization between individual runs.

Downstream data analysis was performed in R version 3.5.1 (2018-07-02). Data were background corrected and normalized using the *normalize_vsn* function (Zhang et al., 2018). Visual inspection of features with missing values showed missing values to be highly biased to specific samples and lower intensity proteins. For this reason, we imputed missing values using random draws from a left-shifted distribution (*impute* function with argument *fun="MinProb", DEP* package). Next, technical replicates were averaged, and differential abundance was tested using the *limma* package (Ritchie et al., 2015). Features with an absolute $\log_2$ fold change > 1 and FDR < 0.05 were considered differentially abundant. Gene ontology (GO) term enrichment analysis was performed using GORILLA (Eden et al., 2009). All significantly upregulated ($\log_2$ fold change > 1 and FDR < 0.05) and all other proteins (background) were entered as two unranked lists and enriched GO molecular function terms were identified by hypergeometric testing. This analysis identified 13 significantly enriched GO molecular groups out of which eight were considered redundant (containing the same group of proteins) and are therefore excluded from Figure 6F.

Quantification and statistical analysis

Statistical analysis of results (apart from mass spectrometry results; see above) was performed using GraphPad Prism 8 (GraphPad Software). Mann-Whitney test for pairwise comparisons (as indicated in the panels) or Mantel-Cox test for survival experiments were applied as indicated in figure legends. *P* values ≤ 0.05 were considered statistically significant. Details regarding statistical analyses of experiments can be found in the respective figure legends. Details regarding data analysis of mass spectrometry experiments can be found in the respective Methods section.

Supplementary Material

Refer to Web version on PubMed Central for supplementary material.

Acknowledgements

We thank members of the Knapp and Galli labs for helpful discussions and Dr. Mindy Tsai also for organizational support. We thank Axel Roers for providing *Mcpt5 Cre* and Hans Oettgen for providing *Igh-7*$^{-/-}$ (IgE-deficient) mice. This work was supported by the Marie Sktodowska-Curie Individual Fellowship (H2020-MSCA-IF-2016 #749629), the European Research Council (ERC-2018-StG #802041) and the INSERM ATIP-Avenir program (to N.G.), the Marie Sktodowska-Curie Individual Fellowship (H2020-MSCA-IF-2014 655153) and the Austrian Science Fund (FWF): P31113-B30 and the Schroedinger Fellowship of the FWF (J3399-B21) (to P.S.) and NIH grants R01 AI23990, R01 AI070813, R01 AR067145 and R01 AI132494 (to S.J.G.). L.L.R. is supported by the INSERM ATIP-Avenir program and the French ANR (grant ANR-18-CE18-0023). T.M. is a Research Associate of the F.R.S.-FNRS and is supported by an "Incentive Grant for Scientific Research" of the F.R.S.-FNRS (grant F.4508.18 to T.M.), by the FRFS-WELBIO (grant CR-2017s-04 to T.M.), by the Acteria Foundation and by an ERC Starting Grant (grant ERC-StG-2018 IM-ID #801823 to T.M.).

References

Akahoshi M, Song CH, Piliponsky AM, Metz M, Guzzetta A, Abrink M, Schlenner SM, Feyerabend TB, Rodewald HR, Pejler G, et al. (2011). Mast cell chymase reduces the toxicity of Gila monster venom, scorpion venom, and vasoactive intestinal polypeptide in mice. The Journal of clinical investigation 121, 4180–4191. [PubMed: 21926462]

Anderson E, Stavenhagen K, Kolarich D, Sommerhoff CP, Maurer M, and Metz M (2018). Human Mast Cell Tryptase Is a Potential Treatment for Snakebite Envenoming Across Multiple Snake Species. Front Immunol 9, 1532. [PubMed: 30038613]

Arifuzzaman M, Mobley YR, Choi HW, Bist P, Salinas CA, Brown ZD, Chen SL, Staats HF, and Abraham SN (2019). MRGPR-mediated activation of local mast cells clears cutaneous bacterial infection and protects against reinfection. Sci Adv 5, eaav0216. [PubMed: 30613778]

Badarau A, Rouha H, Malafa S, Battles MB, Walker L, Nielson N, Dolezilkova I, Teubenbacher A, Banerjee S, Maierhofer B, et al. (2016). Context matters: The importance of dimerization-induced conformation of the LukGH leukocidin of Staphylococcus aureus for the generation of neutralizing antibodies. MAbs 8, 1347–1360. [PubMed: 27467113]

Balbino B, Conde E, Marichal T, Starkl P, and Reber LL (2018). Approaches to target IgE antibodies in allergic diseases. Pharmacol Ther 191, 50–64. [PubMed: 29909239]

Bankhead P, Loughrey MB, Fernandez JA, Dombrowski Y, McArt DG, Dunne PD, McQuaid S, Gray RT, Murray LJ, Coleman HG, et al. (2017). QuPath: Open source software for digital pathology image analysis. Sci Rep 7, 16878. [PubMed: 29203879]

Bruhns P, and Jonsson F (2015). Mouse and human FcR effector functions. Immunol Rev 268, 25–51. [PubMed: 26497511]

Cassini A, Hogberg LD, Plachouras D, Quattrocchi A, Hoxha A, Simonsen GS, Colomb-Cotinat M, Kretzschmar ME, Devleesschauwer B, Cecchini M, et al. (2019). Attributable deaths and disability-adjusted life-years caused by infections with antibiotic-resistant bacteria in the EU and the European Economic Area in 2015: a population-level modelling analysis. Lancet Infect Dis 19, 56–66. [PubMed: 30409683]

Cosmi L, Maggi L, Mazzoni A, Liotta F, and Annunziato F (2019). Biologicals targeting type 2 immunity: Lessons learned from asthma, chronic urticaria and atopic dermatitis. Eur J Immunol 49, 1334–1343. [PubMed: 31355918]

Diep BA, Gill SR, Chang RF, Phan TH, Chen JH, Davidson MG, Lin F, Lin J, Carleton HA, Mongodin EF, et al. (2006). Complete genome sequence of USA300, an epidemic clone of community-acquired meticillin-resistant Staphylococcus aureus. Lancet 367, 731–739. [PubMed: 16517273]

Dombrowicz D, Flamand V, Brigman KK, Koller BH, and Kinet JP (1993). Abolition of anaphylaxis by targeted disruption of the high affinity immunoglobulin E receptor alpha chain gene. Cell 75, 969–976. [PubMed: 8252632]

Eberl G (2016). Immunity by equilibrium. Nat Rev Immunol 16, 524–532. [PubMed: 27396446]

Eden E, Navon R, Steinfeld I, Lipson D, and Yakhini Z (2009). GOrilla: a tool for discovery and visualization of enriched GO terms in ranked gene lists. BMC Bioinformatics 10, 48. [PubMed: 19192299]

Galli SJ, and Tsai M (2012). IgE and mast cells in allergic disease. Nat Med 18, 693–704. [PubMed: 22561833]

Gause WC, Rothlin C, and Loke P (2020). Heterogeneity in the initiation, development and function of type 2 immunity. Nat Rev Immunol.

Gowthaman U, Chen JS, Zhang B, Flynn WF, Lu Y, Song W, Joseph J, Gertie JA, Xu L, Collet MA, et al. (2019). Identification of a T follicular helper cell subset that drives anaphylactic IgE. Science 365.

Hahn BL, and Sohnle PG (2013). Direct translocation of staphylococci from the skin surface to deep organs. Microb Pathog 63, 24–29. [PubMed: 23747685]

Hammad H, and Lambrecht BN (2015). Barrier Epithelial Cells and the Control of Type 2 Immunity. Immunity 43, 29–40. [PubMed: 26200011]

Harris NL, and Loke P (2018). Recent Advances in Type-2-Cell-Mediated Immunity: Insights from Helminth Infection. Immunity 48, 396.

Hughes CS, Foehr S, Garfield DA, Furlong EE, Steinmetz LM, and Krijgsveld J (2014). Ultrasensitive proteome analysis using paramagnetic bead technology. Mol Syst Biol 10, 757. [PubMed: 25358341]

Inoshima I, Inoshima N, Wilke GA, Powers ME, Frank KM, Wang Y, and Bubeck Wardenburg J (2011). A Staphylococcus aureus pore-forming toxin subverts the activity of ADAM10 to cause lethal infection in mice. Nat Med 17, 1310–1314. [PubMed: 21926978]

Kim J, Kim BE, Ahn K, and Leung DYM (2019). Interactions Between Atopic Dermatitis and Staphylococcus aureus Infection: Clinical Implications. Allergy Asthma Immunol Res 11, 593–603. [PubMed: 31332972]

Kobayashi T, Naik S, and Nagao K (2019). Choreographing Immunity in the Skin Epithelial Barrier. Immunity 50, 552–565. [PubMed: 30893586]

Langen U, Schmitz R, and Steppuhn H (2013). [Prevalence of allergic diseases in Germany: results of the German Health Interview and Examination Survey for Adults (DEGS1)]. Bundesgesundheitsblatt Gesundheitsforschung Gesundheitsschutz 56, 698–706. [PubMed: 23703488]

Liu FT, Bohn JW, Ferry EL, Yamamoto H, Molinaro CA, Sherman LA, Klinman NR, and Katz DH (1980). Monoclonal dinitrophenyl-specific murine IgE antibody: preparation, isolation, and characterization. J Immunol 124, 2728–2737. [PubMed: 7373045]

Lloyd CM, and Snelgrove RJ (2018). Type 2 immunity: Expanding our view. Sci Immunol 3.

Marichal T, Gaudenzio N, El Abbas S, Sibilano R, Zurek O, Starkl P, Reber LL, Pirottin D, Kim J, Chambon P, et al. (2016). Guanine nucleotide exchange factor RABGEF1 regulates keratinocyte-intrinsic signaling to maintain skin homeostasis. The Journal of clinical investigation 126, 4497–4515. [PubMed: 27820702]

Marichal T, Starkl P, Reber LL, Kalesnikoff J, Oettgen HC, Tsai M, Metz M, and Galli SJ (2013). A beneficial role for immunoglobulin E in host defense against honeybee venom. Immunity 39, 963–975. [PubMed: 24210352]

Meindl S, Schmidt U, Vaculik C, and Elbe-Burger A (2006). Characterization, isolation, and differentiation of murine skin cells expressing hematopoietic stem cell markers. J Leukoc Biol 80, 816–826. [PubMed: 16864603]

Metz M, Piliponsky AM, Chen CC, Lammel V, Abrink M, Pejler G, Tsai M, and Galli SJ (2006). Mast cells can enhance resistance to snake and honeybee venoms. Science 313, 526–530. [PubMed: 16873664]

Miller LS, and Simon SI (2018). Neutrophils in hot pursuit of MRSA in the lymph nodes. Proceedings of the National Academy of Sciences of the United States of America 115, 2272–2274. [PubMed: 29476009]

Mukai K, Tsai M, Saito H, and Galli SJ (2018). Mast cells as sources of cytokines, chemokines, and growth factors. Immunol Rev 282, 121–150. [PubMed: 29431212]

Mukai K, Tsai M, Starkl P, Marichal T, and Galli SJ (2016). IgE and mast cells in host defense against parasites and venoms. Semin Immunopathol 38, 581–603. [PubMed: 27225312]

Musher DM, and Thorner AR (2014). Community-acquired pneumonia. N Engl J Med 371, 1619–1628. [PubMed: 25337751]

Nakamura Y, Oscherwitz J, Cease KB, Chan SM, Munoz-Planillo R, Hasegawa M, Villaruz AE, Cheung GY, McGavin MJ, Travers JB, et al. (2013). Staphylococcus delta-toxin induces allergic skin disease by activating mast cells. Nature 503, 397–401. [PubMed: 24172897]

Oettgen HC (2016). Fifty years later: Emerging functions of IgE antibodies in host defense, immune regulation, and allergic diseases. J Allergy Clin Immunol 137, 1631–1645. [PubMed: 27263999]

Oettgen HC, Martin TR, Wynshaw-Boris A, Deng C, Drazen JM, and Leder P (1994). Active anaphylaxis in IgE-deficient mice. Nature 370, 367–370. [PubMed: 8047141]

Olsen JV, de Godoy LM, Li G, Macek B, Mortensen P, Pesch R, Makarov A, Lange O, Horning S, and Mann M (2005). Parts per million mass accuracy on an Orbitrap mass spectrometer via lock mass injection into a C-trap. Mol Cell Proteomics 4, 2010–2021. [PubMed: 16249172]

Otto M (2014). Staphylococcus aureus toxins. Current opinion in microbiology 17, 32–37. [PubMed: 24581690]

Palm NW, Rosenstein RK, and Medzhitov R (2012). Allergic host defences. Nature 484, 465–472. [PubMed: 22538607]

Palm NW, Rosenstein RK, Yu S, Schenten DD, Florsheim E, and Medzhitov R (2013). Bee venom phospholipase A2 induces a primary type 2 response that is dependent on the receptor ST2 and confers protective immunity. Immunity 39, 976–985. [PubMed: 24210353]

Perez-Riverol Y, Csordas A, Bai J, Bernal-Llinares M, Hewapathirana S, Kundu DJ, Inuganti A, Griss J, Mayer G, Eisenacher M, et al. (2019). The PRIDE database and related tools and resources in 2019: improving support for quantification data. Nucleic Acids Res 47, D442–D450. [PubMed: 30395289]

Piliponsky AM, and Romani L (2018). The contribution of mast cells to bacterial and fungal infection immunity. Immunol Rev 282, 188–197. [PubMed: 29431211]

Popov LM, Marceau CD, Starkl PM, Lumb JH, Shah J, Guerrera D, Cooper RL, Merakou C, Bouley DM, Meng W, et al. (2015). The adherens junctions control susceptibility to Staphylococcus aureus alpha-toxin. Proceedings of the National Academy of Sciences of the United States of America 112, 14337–14342. [PubMed: 26489655]

Prabhakara R, Foreman O, De Pascalis R, Lee GM, Plaut RD, Kim SY, Stibitz S, Elkins KL, and Merkel TJ (2013). Epicutaneous model of community-acquired Staphylococcus aureus skin infections. Infect Immun 81, 1306–1315. [PubMed: 23381997]

Profet M (1991). The function of allergy: immunological defense against toxins. The Quarterly review of biology 66, 23–62. [PubMed: 2052671]

Pundir P, Liu R, Vasavda C, Serhan N, Limjunyawong N, Yee R, Zhan Y, Dong X, Wu X, Zhang Y, et al. (2019). A Connective Tissue Mast-Cell-Specific Receptor Detects Bacterial Quorum-Sensing Molecules and Mediates Antibacterial Immunity. Cell Host Microbe 26, 114–122 e118. [PubMed: 31278040]

Reber LL, Hernandez JD, and Galli SJ (2017). The pathophysiology of anaphylaxis. J Allergy Clin Immunol 140, 335–348. [PubMed: 28780941]

Redegeld FA, Yu Y, Kumari S, Charles N, and Blank U (2018). Non-IgE mediated mast cell activation. Immunol Rev 282, 87–113. [PubMed: 29431205]

Ritchie ME, Phipson B, Wu D, Hu Y, Law CW, Shi W, and Smyth GK (2015). limma powers differential expression analyses for RNA-sequencing and microarray studies. Nucleic Acids Res 43, e47. [PubMed: 25605792]

Rouha H, Weber S, Janesch P, Maierhofer B, Gross K, Dolezilkova I, Mirkina I, Visram ZC, Malafa S, Stulik L, et al. (2018). Disarming Staphylococcus aureus from destroying human cells by simultaneously neutralizing six cytotoxins with two human monoclonal antibodies. Virulence 9, 231–247. [PubMed: 29099326]

Rudkin JK, McLoughlin RM, Preston A, and Massey RC (2017). Bacterial toxins: Offensive, defensive, or something else altogether? PLoS Pathog 13, e1006452. [PubMed: 28934339]

Schneider LA, Schlenner SM, Feyerabend TB, Wunderlin M, and Rodewald HR (2007). Molecular mechanism of mast cell mediated innate defense against endothelin and snake venom sarafotoxin. J Exp Med 204, 2629–2639. [PubMed: 17923505]

Scholten J, Hartmann K, Gerbaulet A, Krieg T, Muller W, Testa G, and Roers A (2008). Mast cell-specific Cre/loxP-mediated recombination in vivo. Transgenic Res 17, 307–315. [PubMed: 17972156]

Sintobin I, Siroux V, Holtappels G, Pison C, Nadif R, Bousquet J, and Bachert C (2019). Sensitisation to staphylococcal enterotoxins and asthma severity: a longitudinal study in the EGEA cohort. Eur Respir J 54.

Stapels DA, Geisbrecht BV, and Rooijakkers SH (2015). Neutrophil serine proteases in antibacterial defense. Current opinion in microbiology 23, 42–48. [PubMed: 25461571]

Starkl P, Marichal T, Gaudenzio N, Reber LL, Sibilano R, Tsai M, and Galli SJ (2016). IgE antibodies, FcepsilonRIalpha, and IgE-mediated local anaphylaxis can limit snake venom toxicity. J Allergy Clin Immunol 137, 246–257 e211. [PubMed: 26410782]

Stemeseder T, Klinglmayr E, Moser S, Lueftenegger L, Lang R, Himly M, Oostingh GJ, Zumbach J, Bathke AC, Hawranek T, and Gadermaier G (2017). Cross-sectional study on allergic sensitization of Austrian adolescents using molecule-based IgE profiling. Allergy 72, 754–763. [PubMed: 27753449]

Stentzel S, Teufelberger A, Nordengrun M, Kolata J, Schmidt F, van Crombruggen K, Michalik S, Kumpfmuller J, Tischer S, Schweder T, et al. (2017). Staphylococcal serine protease-like proteins are pacemakers of allergic airway reactions to Staphylococcus aureus. J Allergy Clin Immunol 139, 492–500 e498. [PubMed: 27315768]

Stryjewski ME, and Chambers HF (2008). Skin and soft-tissue infections caused by community-acquired methicillin-resistant Staphylococcus aureus. Clin Infect Dis 46 Suppl 5, S368–377. [PubMed: 18462092]

Sullivan BM, Liang HE, Bando JK, Wu D, Cheng LE, McKerrow JK, Allen CD, and Locksley RM (2011). Genetic analysis of basophil function in vivo. Nat Immunol 12, 527–535. [PubMed: 21552267]

Takai T, Li M, Sylvestre D, Clynes R, and Ravetch JV (1994). FcR gamma chain deletion results in pleiotrophic effector cell defects. Cell 76, 519–529. [PubMed: 8313472]

Torres A, and Rello J (2010). Update in community-acquired and nosocomial pneumonia 2009. Am J Respir Crit Care Med 181, 782–787. [PubMed: 20382801]

Untersmayr E, Diesner SC, Oostingh GJ, Selzle K, Pfaller T, Schultz C, Zhang Y, Krishnamurthy D, Starkl P, Knittelfelder R, et al. (2010). Nitration of the egg-allergen ovalbumin enhances protein allergenicity but reduces the risk for oral sensitization in a murine model of food allergy. PLoS One 5, e14210. [PubMed: 21151984]

Van Zele T, Gevaert P, Watelet JB, Claeys G, Holtappels G, Claeys C, van Cauwenberge P, and Bachert C (2004). Staphylococcus aureus colonization and IgE antibody formation to enterotoxins is increased in nasal polyposis. J Allergy Clin Immunol 114, 981–983. [PubMed: 15480349]

Voehringer D (2013). Protective and pathological roles of mast cells and basophils. Nat Rev Immunol 13, 362–375. [PubMed: 23558889]

Voehringer D, Liang HE, and Locksley RM (2008). Homeostasis and effector function of lymphopenia-induced “memory-like” T cells in constitutively T cell-depleted mice. J Immunol 180, 4742–4753. [PubMed: 18354198]

Walch M, Dotiwala F, Mulik S, Thiery J, Kirchhausen T, Clayberger C, Krensky AM, Martinvalet D, and Lieberman J (2014). Cytotoxic cells kill intracellular bacteria through granulysin-mediated delivery of granzymes. Cell 157, 1309–1323. [PubMed: 24906149]

Wernersson S, and Pejler G (2014). Mast cell secretory granules: armed for battle. Nat Rev Immunol 14, 478–494. [PubMed: 24903914]

Zhang X, Smits AH, van Tilburg GB, Ovaa H, Huber W, and Vermeulen M (2018). Proteome-wide identification of ubiquitin interactions using UbIA-MS. Nat Protoc 13, 530–550. [PubMed: 29446774]

Highlights

- *Staphylococcus aureus* skin infection leads to specifc and functional IgE antibodies
- Skin initiated immunity protects against secondary lung and skin infections
- Mast cells and IgE antibodies play key roles in acquired resistance to *S. aureus*
- IgE-activated mast cells interfere with *S. aureus* growth and toxicity

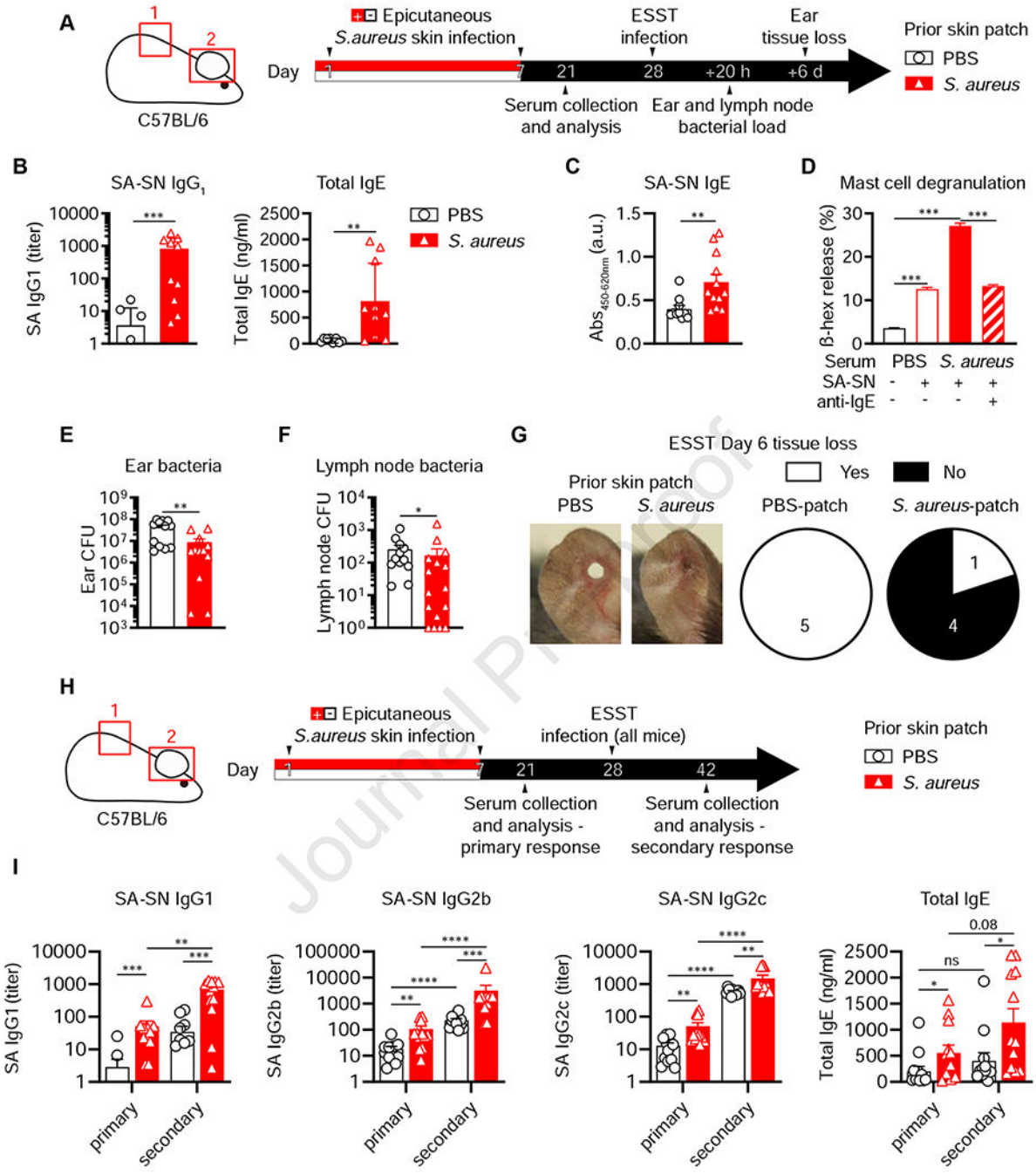

Figure 1:

Skin-initiated immunity increases host defense against severe soft tissue infection with SA (**A**) Experimental scheme for B to G. (**B**) Day 21 serum amounts of SA culture supernatant (SA-SN)-specific IgG1 (SA-SN IgG1) and total IgE antibodies. (**C**) Day 21 serum amounts of SA-SN-specific IgE (SA-SN IgE). (**D**) Degranulation (% ß-hexosaminidase release) upon SA-SN exposure of fetal skin-derived cultured mast cells (FSCMCs) sensitized with untreated or anti-IgE-treated serum from PBS or SA-infected animals. (E and F) Bacterial colony forming units (CFUs) in (**D**) ear and (**E**) draining cervical lymph nodes 20 hours

after ear skin and soft tissue (ESST) infection. (**G**) Mice with ear tissue loss on day 6 after ESST infection and representative (of two independent experiments) pictures. (**H**) Experimental scheme for (I). (**I**) Day 21 (primary immune response) and day 42 (secondary immune response) serum amounts of SA-SN-specific IgG1, IgG2b, IgG2c (SA-SN IgG1 IgG2b, IgG2c, respectively) and total IgE antibodies. (B to F, I): Mann-Whitney Test for indicated pairwise comparisons; symbols represent biological replicates; (B): n=9-10 (only mock-infected samples with an IgG1 titer ≥ 1 are shown); (C): n=10-12; (E and F): n=12-16; (G): n=5; (I): n=12 (only mock-infected samples with an IgG1 titer ≥ 1 are shown); data shown were pooled from two independent experiments, except for (D), which are from one experiment (representative of two independent experiments). ns (not significant); *P ≤ 0.05; **P ≤ 0.01; ***P ≤ 0.001. Error bars represent mean +SEM apart from (D) where they represent mean +SD. Please also see Figure S1.

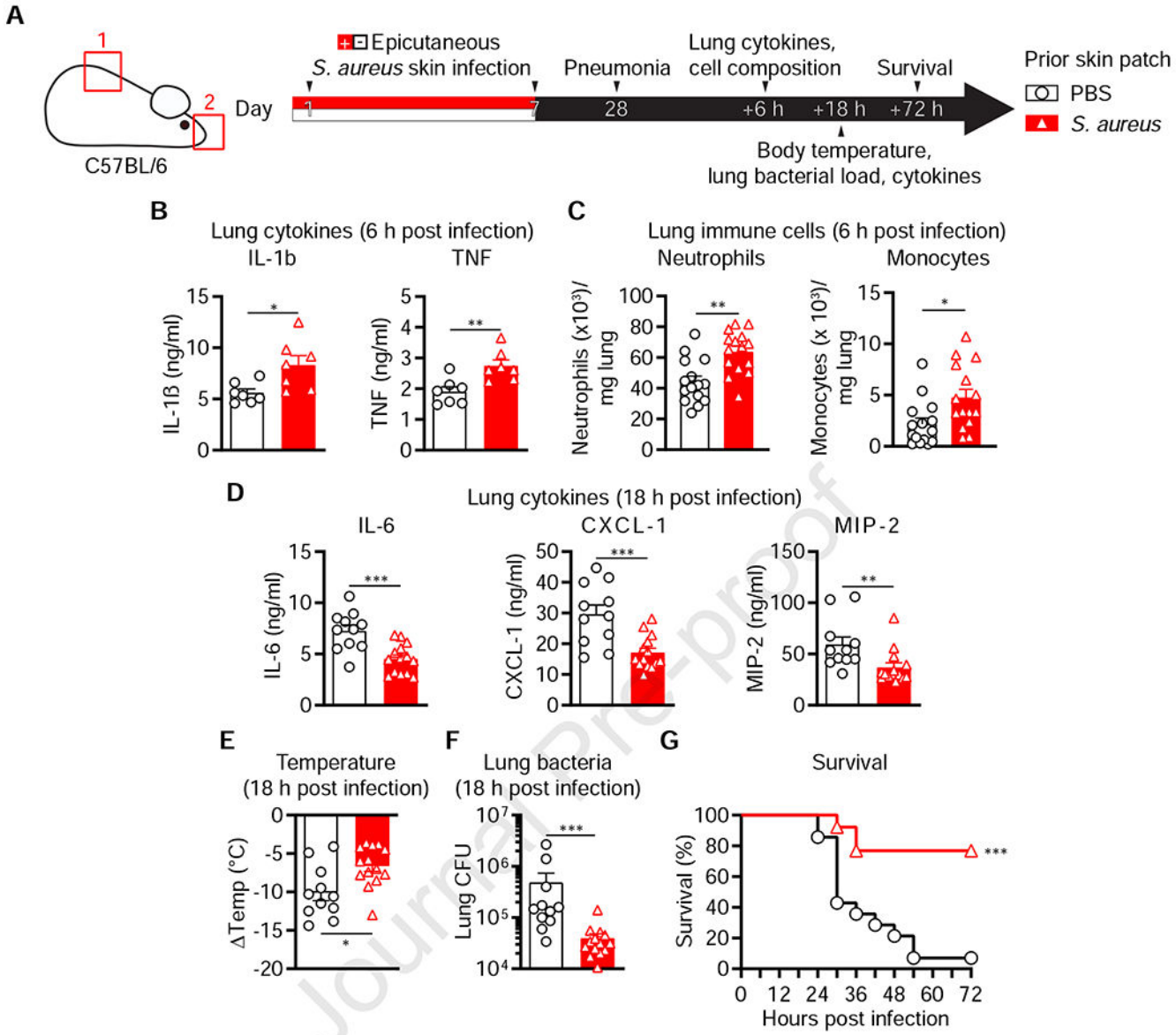

Figure 2:

Prior skin infection improves host defense against SA pneumonia

(**A**) Experimental scheme for B to G. (**B**) Lung tissue cytokine amounts 6 hours after infection. (**C**) Lung immune cell counts (by flow cytometry) 6 hours after infection (also see Figure S2 for gating strategy and additional cell types). (**D**) lung (homogenate) cytokine amounts (**E**) body temperature, and (**F**) lung tissue CFUs 18 hours after infection. (**G**) Survival after intranasal infection. (C to G): Mann-Whitney Test for indicated pairwise comparisons; symbols represent biological replicates; (G): Mantel-Cox test; (G): n=13-14; (B to E): n=11-14; (B): n=7; (C): n=15; *P ≤ 0.05; **P ≤ 0.01; ***P ≤ 0.001. Error bars represent mean + or −SEM apart from (F) where they represent mean +SD. Please also see Figure S2.

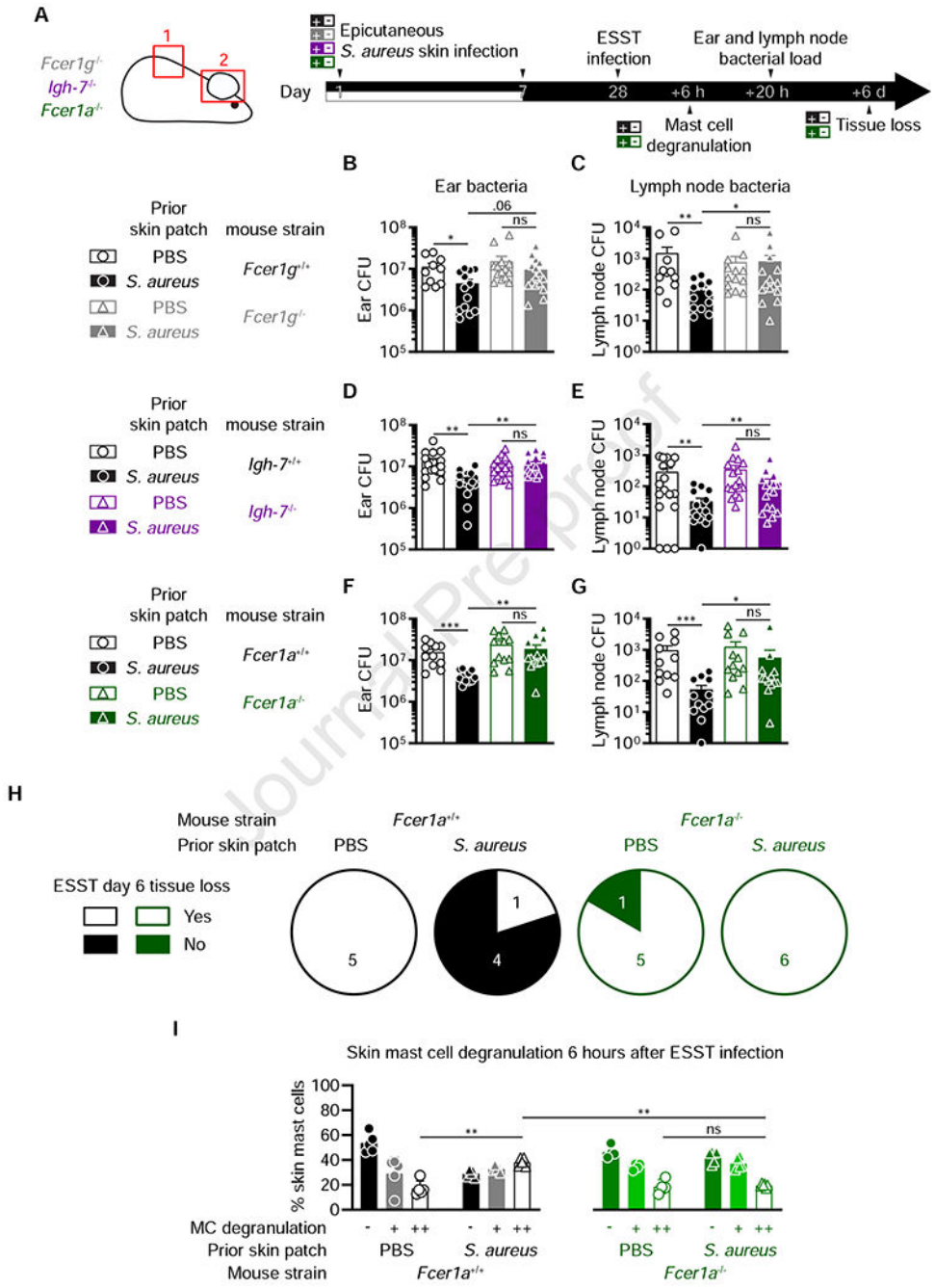

Figure 3:

Acquired immunity against SA requires functional IgE effector mechanisms

(**A**) Experimental scheme for B to I. (**B** to **G**) Bacterial colony forming units (CFUs) in (B, D and F) ears and (C, E and G) draining (cervical) lymph nodes 20 hours after ear skin and soft tissue (ESST) infection. (**H**) Mice with ear tissue loss on day 6 after ESST infection. (**I**) Quantification of none (−), moderately (+) and extensively (++) degranulated mast cells in whole ear tissue sections 6 hours after ESST infection. (B to G, I): Mann-Whitney Test for indicated pairwise comparisons; symbols represent values from single mice; (B): data were

pooled from two independent experiments. (I): data are from one experiment (representative of two independent experiments). (B and C) n=10-16; (D and E) n=17-18; (F and G) n=11-13; ns (not significant); (H) n=5-6; (I) n=4-6; ns (not significant); *P ≤ 0.05; **P ≤ 0.01; ***P ≤ 0.001. Error bars represent (B to G) mean +SEM or (I) mean +SD. Please also see Figure S3.

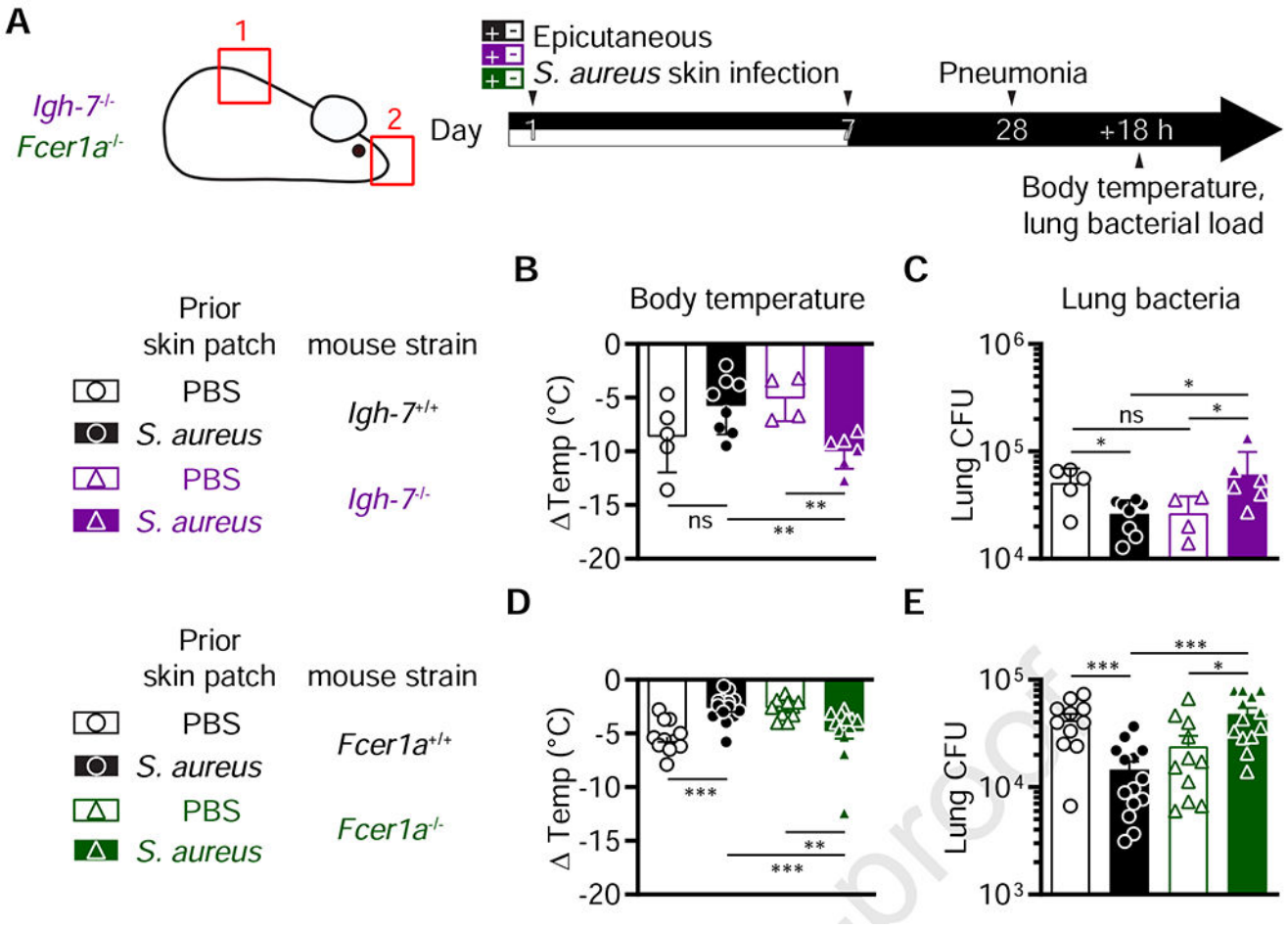

Figure 4:

IgE effector mechanisms contribute to acquired immunity against SA pneumonia

(**A**) Experimental scheme for B to E. (**B** and **D**) Body temperature and (**C** and **E**) lung tissue bacterial colony forming units (CFUs) 18 hours after intranasal infection. (B to E): Mann-Whitney Test for indicated pairwise comparisons; symbols represent values from single mice; (D and E): data were pooled from two independent experiments. (D and E) n=11-14; (B and C) data shown are from one experiment; n=4-8. ns (not significant); *P ≤ 0.05; **P ≤ 0.01; ***P ≤ 0.001. Error bars represent (D and E) mean + or − SEM or (B and C) mean + or − SD.

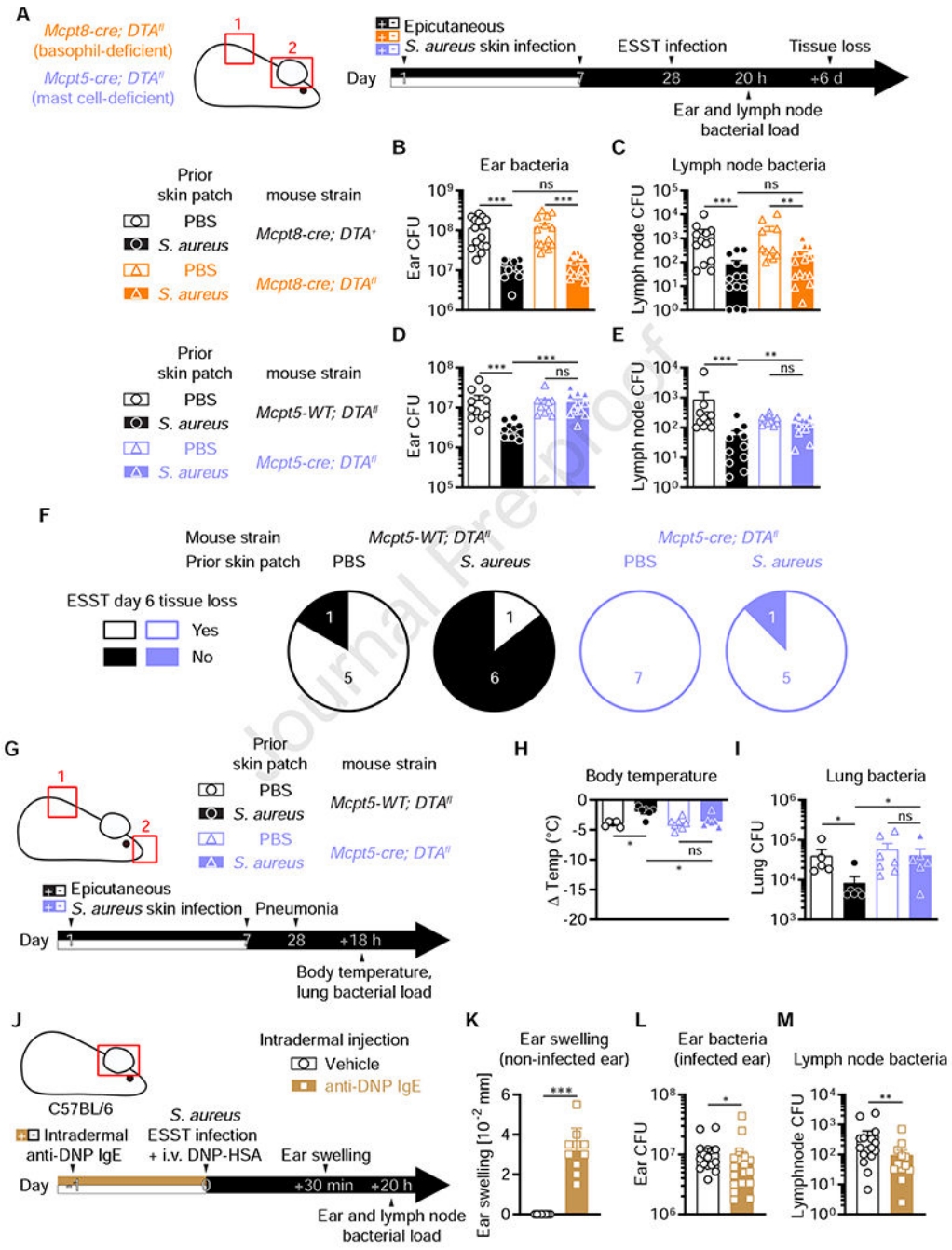

Figure 5:

MCs and local allergic reactions can contribute to anti-SA immunity

(**A**) Experimental scheme for B to E. (**B** to **E**) Bacterial colony forming units (CFUs) in the (B and D) ears and (C and E) draining (cervical) lymph nodes 20 hours after ear skin and soft tissue (ESST) infection. (**F**) Mice with ear tissue loss on day 6 after ESST infection. (**G**) Experimental scheme for H and I. (**H**) Body temperature and (**I**) lung tissue bacterial CFUs 18 hours after intranasal infection. (**J**) Experimental scheme for K to M. (**K**) Ear swelling 30 minutes after dinitrophenyl-labelled human serum albumin (DNP-HSA) injection in mice

that received anti-DNP IgE the day before. (**L** and **M**) Bacterial load in (L) ear and (M) draining lymph nodes 20 hours after ESST infection and DNP-HSA injection. (B to E, H, I, K-M): Mann-Whitney Test for indicated pairwise comparisons; all graphs show data pooled from two independent experiments apart from H and I which depict results of one experiment; symbols represent values from single mice; (B and C) n=14-15; (D and E) n=10-12; (F) n=5-7; (H and I) n=5-7; (K) n=10-11; (L and M) n=16-18. ns (not significant); *P ≤ 0.05; **P ≤ 0.01; ***P ≤ 0.001. Error bars represent mean +SEM. Please also see Figure S4.

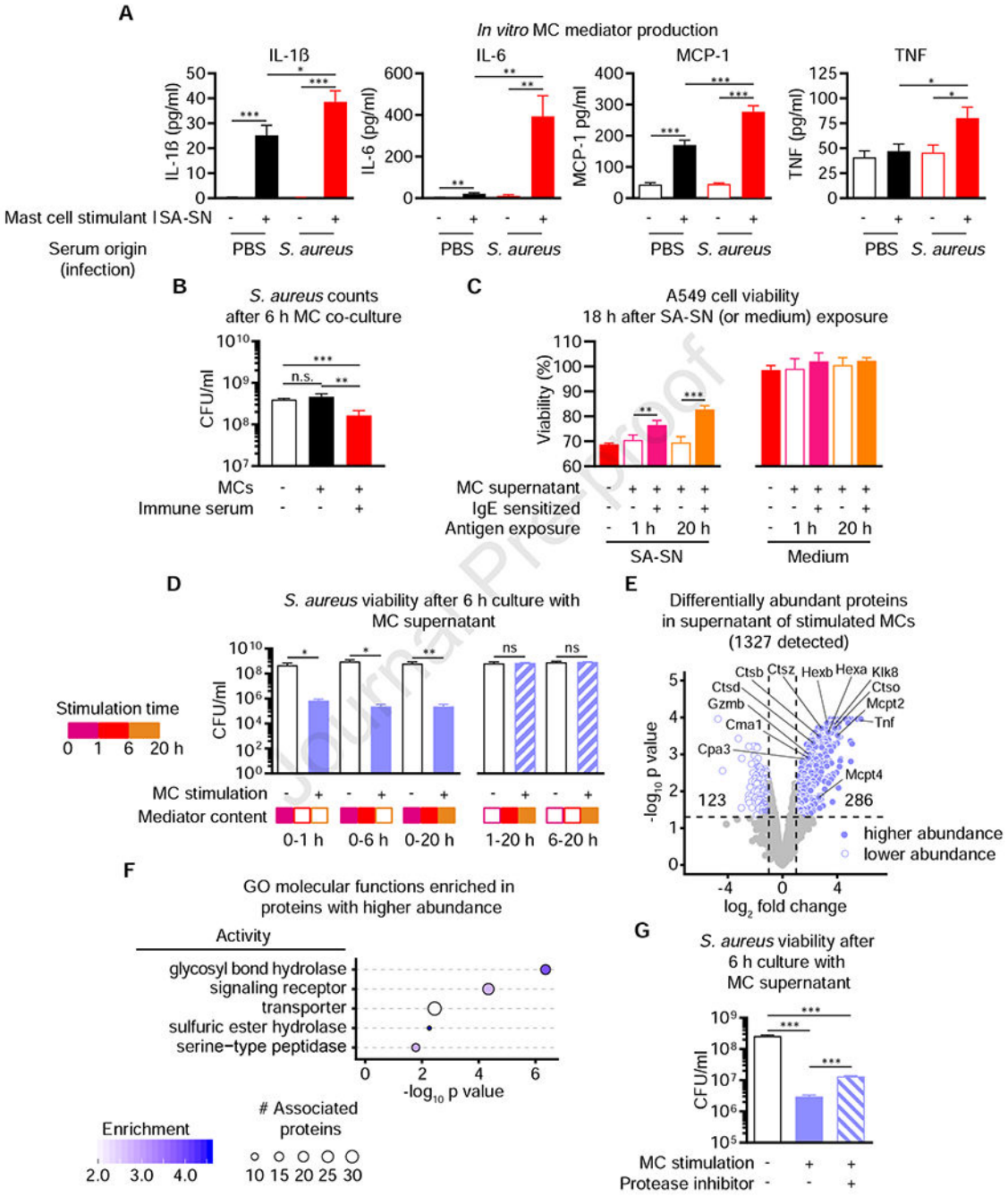

Figure 6:

IgE-activated MCs counteract SA toxicity and amplification

(**A**) Cytokine production of fetal skin-derived cultured mast cells (FSCMCs) sensitized with serum from mice with prior epicutaneous SA or mock infection upon exposure to SA culture supernatant (SA-SN) for 18 hours. (**B**) SA viability after 6 hours co-culture with or without FSCMCs pre-sensitized or not with immune serum collected from mice three weeks after epicutaneous back skin infection. (**C**) Viability (% of untreated cells) of A549 lung epithelial cells after 18 hours exposure to SA-SN (left panel) or plain bacterial culture medium (right

panel) which was either untreated or pre-incubated with supernatant collected from anti-dinitrophenyl (DNP) IgE-sensitized or non-sensitized FSCMCs 1 h or 20 h after DNP-labelled human serum albumin (DNP-HSA) stimulation. (**D**) SA viability after 6 hours culture in presence of supernatant of FSCMCs that were stimulated (or not) with IgE and antigen, containing mediators released over one (0-1 h), six (0-6 h) or 20 hours (0-20 h) (left panel). Right panel: bacterial viability upon culture with supernatant from mast cells from which supernatant was removed after 1 hour (1-20 h) or 6 hours (6-20 h), followed by addition of fresh medium and antigen for the remaining time. (**E**) Volcano plot depicting mass spectrometry results of SN collected 1 h after DNP-HSA exposure of anti-DNP IgE-sensitized or non-sensitized FSCMCs. Significantly up-regulated data points (blue circles) with potential antibacterial function are annotated. (**F**) Enriched GO term molecular functions among up-regulated proteins (see E). (**G**) SA viability 6 hours after culture with SN from non-stimulated or IgE- and antigen- (1 hour) stimulated FSCMCs. Supernatant of stimulated cells was optionally treated with protease inhibitor. (A to D, G): Mann-Whitney Test for indicated pairwise comparisons; (A to D, G): Data are representative of at least two independent experiments. (E and F) Data are representative of one analysis of sample triplicates analyzed in duplicate. ns (not significant); *P ≤ 0.05; **P ≤ 0.01; ***P ≤ 0.001. (A to D, G) Error bars represent mean +SD. Please also see Figure S5.

KEY RESOURCES TABLE

REAGENT or RESOURCE	SOURCE	IDENTIFIER
Antibodies		
Anti-dinitrophenyl (DNP) IgE	Fu-Tong Liu; (Liu et al., 1980)	N/A
TruStain FcX (anti-mouse CD16/32)	BioLegend	101319
eBioscience Fixable Viability Dye eFluor 780	Thermo Fisher Scientific	65-0865-14
Brilliant Violet 510 anti-mouse CD45	BioLegend	103137
PE/Cy7 anti-mouse F4/80	BioLegend	123113
Alexa Fluor 700 anti-mouse CD11b	BioLegend	101222
PerCP Cy5.5 anti-mouse/human CD11c	BioLegend	117327
Brilliant Violet 605 anti-mouse CD19	BioLegend	115539
Brilliant Violet 605 anti-mouse Ly6c	BioLegend	128035
PE/Cy7 anti-mouse Ly6g	BioLegend	127317
Alexa Fluor 647 anti-mouse Siglec F	BD Pharmingen	562680
FITC anti-mouse CD3	BioLegend	100203
PE/Dazzle anti-mouse CD3	BioLegend	100245
Alexa Fluor 700 anti-mouse CD4	BioLegend	100536
PerCP Cy5.5 anti-mouse CD4	BioLegend	100433
PE/Cy7 anti-mouse CD8a	BioLegend	100721
PE/Dazzle anti-mouse CD8a	BioLegend	100761
Alexa Fluor 700 anti-mouse CD8a	BioLegend	100729
APC anti-mouse NK1.1	BioLegend	108709
PE anti-mouse CD335 (NKp46)	BioLegend	137603
PE anti-mouse FcεRIα	BioLegend	134307
Pacific Blue anti-mouse CD117 (c-Kit)	BioLegend	105819
Brilliant Violet 605 anti-mouse CXCR5	BioLegend	145513
Brilliant Violet 421 anti-mouse PD-1	BioLegend	109121
FITC anti-mouse CD44	BioLegend	103022
PE Cy7 anti-mouse IL-4	BioLegend	504117
APC anti-mouse IL-5	BioLegend	504305
PE anti-mouse IL-13	eBioscience	7133-12-01
Anti-mouse IgE (clone 35-92)	BD Pharmingen	553416
Rat IgG1 isotype control (clone R3-34)	BD Pharmingen	553922
Biotin anti-mouse IgG1	BD Pharmingen	550331
Biotin anti-mouse IgG2b	BD Pharmingen	553393
Biotin anti-mouse IgG2c	Southern Biotech	1079-08
Anti-mouse IgE (clone R35-72)	BD Pharmingen	553413
Biotin anti-mouse IgE	BD Pharmingen	553419
Mouse IgE	BD Pharmingen	557079

REAGENT or RESOURCE	SOURCE	IDENTIFIER
Bacterial and Virus Strains		
Staphylococcus aureus; strain USA300	Fabio Bagnoli (Popov et al., 2015)	
Staphylococcus aureus; strain TCH1516	ATCC	BAA-1717
Staphylococcus aureus; strain TCH1516 Δ*hla/hlgABC/lukSF/lukED/lukGH*	Lukas Stulik (Badarau et al., 2016; Rouha et al., 2018)	
Chemicals, Peptides, and Recombinant Proteins		
Recombinant mouse interleukin-3	Peprotech	213-13
Recombinant mouse stem cell factor	Peprotech	250-03
Collagenase I	Gibco/Thermo Fisher Scientific	17018029
DNase I	Sigma	DN25
CellTrace CFSE Cell Proliferation Kit	Invitrogen/Thermo Fisher Scientific	C34554
Phorbol 12-myristate 13-acetate	Sigma	P8139
Ionomycin	Sigma	I0634
GolgiStop	BD Biosciences	554724
4-Nitrophenyl N-acetyl-ß-D-galactosaminide	Sigma	N9003
Dinitrophenyl-labelled human serum albumin (DNP-HSA)	Sigma	A6661
cOmplete Mini EDTA Free Protease Inhibitor Cocktail	Roche	4693159001
Critical Commercial Assays		
Mouse IL-6 ready-SET-Go! Kit	Fischer Scientific	501128696
Mouse IL-13 ready-SET-Go! Kit	Fischer Scientific	501128703
Mouse CXCL1/KC DuoSet ELISA	R&D Systems	DY453-05
Mouse CXCL2/MIP-2 Quantikine ELISA Kit	R&D Systems	MM200
CellTiter-Glo Luminescent Cell Viability Assay	Promega	G7570
Mouse Th1/Th2/Th17 Cytokine Kit	BD Biosciences	560485
Procarta Mix&Match 11plex	Thermo Fisher Scientific	ppx-11-mxgzfag
High-Capacity cDNA Reverse Transcription Kit	Thermo Fisher Scientific	4368814
Power SYBR Green PCR Master Mix	Thermo Fisher Scientific	4367659
Deposited Data		
Mast cell secretome mass spectrometry data	ProteomXchange (Perez-Riverol et al., 2019)	Project accession: PXD019107 Project DOI: 10.6019/ PXD019107
Experimental Models: Organisms/Strains		
Mouse/C57BL/6J	Own colony, Jackson Labs	JAX #000664
Mouse/Tg(Cma1-cre)Aroer	Axel Roers; (Scholten et al., 2008)	MGI ID: 3785000
B6.129S4-*Mcpt8*$^{tm1(cre)Lky}$/J	Jackson Labs; (Sullivan et al., 2011)	JAX #017578
B6.129P2-*Gt(ROSA)26*$^{Sortm1(DTA)Lky}$/J	Jackson Labs; (Voehringer et al., 2008)	JAX #009669
B6.129S2(Cg)-*Fcer1a*^{tm1Knt}/J	Jackson Labs; (Dombrowicz et al., 1993)	JAX #010512
B6.129P2-*Fcer1g*^{tm1Rav} N12	Taconic; (Takai et al., 1994)	Model 584

REAGENT or RESOURCE	SOURCE	IDENTIFIER
Igh-7^{tm1Led}	Hans Oettgen; (Oettgen et al., 1994)	MGI ID: 2387579
Oligonucleotides		
Mouse *Eef1b2*: fwd: AGAGCTACATTGAGGGGTACGT; rev: GACTTGATGTGATTATACCAACGTAG	(Marichal et al., 2016)	N/A
Mouse *il1b*: fwd: GCTTCCTTGTGCAAGTGTCTGAA; rev: GAACAGGTCATTCTCATCACTGTCA;	(Marichal et al., 2016)	N/A
Mouse *il4*: fwd: GTCCTCACAGCAACGAAGAACACCA; rev: CTCATTCATGGTGCAGCTTATCGA;	(Marichal et al., 2016)	N/A
Mouse *il6*: fwd: GAAGTTCCTCTCTGCAAGAGAC; rev: GTATCCTCTGTGAAGTCTCCTCT;	This paper	N/A
Mouse *il13*: fwd: TATTGAGGAGCTGAGCAACATCAC; rev: TCTGGGTCCTGTAGATGGCA;	(Untersmayr et al., 2010)	N/A
Mouse *il17a*: fwd: GAGAGCTTCATCTGTGTCTCTGAT; rev: TCAGTGTTTGGACACGCTGAGCT;	(Marichal et al., 2016)	N/A
Mouse *ccl2*: fwd: AAGCTGTAGTTTTTGTCACCAAG; rev: CCATTTGGTTCCGATCCAGGTTT;	This paper	N/A
Mouse *ccl3/mip1a*: fwd: CTCTGTACCATGACACTCTGCA; rev: CTCTTAGTCAGGAAAATGACACCTG;	(Marichal et al., 2016)	N/A
Mouse *ccl4*: fwd: GTTCTCAGCACCAATGGGCTCTGA; rev: AGCAAAGACTGCTGGTCTCATAGTA;	This paper	N/A
Mouse *ccl5*: fwd: CCACGTCAAGGAGTATTTCTACACCA; rev: GTTCCTTCGAGTGACAAACACGACT;	This paper	N/A
Mouse *ccl8*: fwd: GAAGCTGTGGTTTTCCAGACCA; rev: CTGGTCAAGGATCTCCATGTAC;	This paper	N/A
Mouse *cxcl1*: fwd: AATGAGCTGCGCTGTCAGTGCCTG; rev: ACCATTCTTGAGTGTGGCTATGACT;	(Marichal et al., 2016)	N/A
Mouse *cxcl2/mip2*: fwd: GTGAACTGCGCTGTCAATGCCTGA; rev: CTTGAGAGTGGCTATGACTTCTGTCT;	This paper	N/A
Mouse *ifng*: fwd: TGAGGTCAACAACCCACAGG; rev: TTCCGCTTCCTGAGGCTGGA;	(Marichal et al., 2016)	N/A
Mouse *tnf*: fwd: GAACTGGCAGAAGAGGCACT; rev: GGTCTGGGCCATAGAACTGA;	This paper	N/A
Software and Algorithms		
FlowJo	FlowJo LLC	v10.5.0.
Graphpad Prism	Graphpad Software	v8
Proteome Discoverer	Thermo Fisher Scientific	v2.2.0.388
QuPath	(Bankhead et al., 2017)	V0.2.0
R	r-project	v3.5.1
Normalize_vsn	(Zhang et al., 2018)	
Limma	(Ritchie et al., 2015)	
GORILLA	(Eden et al., 2009)	
Other		
Morrow Brown allergy prick test needles	Morrow Brown Allergy Diagnostics	MB-2000
3M Tegaderm Transparent Film Roll	3M	16004
Dial Thickness Gauge G-1a	Peacock Ozaki	N/A

REAGENT or RESOURCE	SOURCE	IDENTIFIER
Fix and Perm Cell Fixation and Permeabilization Kit	Nordic MUbio/Thermo Fisher Scientific	GAS004
Fixation/Permeabilization Solution Kit	BD Biosciences	554714